Bioresources and Bioproducts

MDPI

Article

Radial Variability in Bamboo Properties: Implications for Sustainable Biochar Production and Agricultural Applications

Krisnna Sousa Alves, Tiago Guimarães *, Angélica de Cássia Oliveira Carneiro, Ana Márcia Macedo Ladeira Carvalho, Sebastião Renato Valverde and Marcelo Moreira da Costa

Department of Forestry Engineering, Federal University of Viçosa, Viçosa 36570-900, MG, Brazil; krisnna.alves@ufv.br (K.S.A.); cassiacarneiro1@gmail.com (A.d.C.O.C.); ana.marcia@ufv.br (A.M.M.L.C.); valverde@ufv.br (S.R.V.); mmdc@ufv.br (M.M.d.C.)

* Correspondence: tguimaraes.quimica@gmail.com

Abstract

Anatomical, chemical, and physical properties are critical for optimizing bamboo applications. This study evaluated the radial variability of these properties in four bamboo species (*Guadua chacoensis*, *Dendrocalamus strictus*, *Bambusa nutans*, and *Dendrocalamus asper*) to assess their potential as sustainable raw materials. Anatomical analysis revealed significant radial gradients: fiber wall thickness and lignin content peaked in the peripheral region (e.g., 30.40% lignin in *D. strictus*), while carbohydrate content was highest in the central region (69.15% in *D. asper*). Basic density varied radially, with the highest values in *G. chacoensis* (835 kg/m^3) and *B. nutans* (858 kg/m^3). Principal Component Analysis (PCA) identified density and chemical composition as key discriminators among species. *Dendrocalamus strictus* emerged as the most promising species for biochar production, exhibiting high gravimetric yield (31.14%), thermal stability, and a mesoporous structure (120.154 m^2/g surface area). The biochar's high elemental carbon (89.66%), calculated fixed carbon (84.97%), crystallinity index (30.16%), and low volatile content (6.83%) suggest potential for use as a soil conditioner for carbon sequestration, although direct agronomic validation (e.g., soil, plant, or microbial assays) is still required. A techno-economic assessment (TEA) demonstrated its commercial viability, projected a profit of approximately US$ 89/ton and US$ 1107/hectare per year under a 3-year rotation cycle, assuming a unified market price of US$ 120/ton. This estimate is preliminary and does not include sensitivity analysis, which is suggested for future work. This study underscores *D. strictus* as a dual-purpose resource, combining ecological benefits (e.g., soil enhancement) with economic feasibility, advancing sustainable agro-industrial applications of bamboo.

Keywords: bamboo radial variability; biochar characterization; techno-economic analysis; sustainable agriculture; lignocellulosic biomass

Academic Editor: Carlos Afonso Teixeira

Received: 27 April 2026
Revised: 25 May 2026
Accepted: 1 June 2026
Published: 4 June 2026

1. Introduction

With the increasing demand for eco-friendly alternatives, bamboo stands out as a viable and sustainable option [1]. This versatile plant has garnered growing interest across various research fields, ranging from civil construction to furniture production, pulp, paper, bioenergy, and handicrafts [2]. In Brazil, the diversity of native bamboo species offers significant potential for economic and environmentally sustainable exploitation [3]. Current literature highlights the versatility of bamboo, underscoring its relevance in both traditional and innovative contexts [4].

Bamboo is an abundant natural resource covering approximately 35 million hectares of forests worldwide [5]. It is highly valued for its rapid growth rate, early maturity, and broad climatic adaptability [6]. These characteristics not only make bamboo ideal for cultivation but also contribute significantly to oxygenation and carbon dioxide capture from the environment, playing a crucial role in mitigating climate change [7].

Globally, the distribution of bamboo species occurs across the Americas, Africa, and Asia, with some species recently introduced in Europe [8]. Among American countries, Brazil has the greatest diversity of species, with the largest areas found in the Amazon and Atlantic forests. In Brazil, the Olyreae and Bambuseae tribes are present, currently comprising 258 native species and 35 genera [9]. The Olyreae tribe consists of herbaceous bamboos with 17 genera and 93 species. The Bambuseae tribe includes 18 genera and 165 species, consisting of lignified or woody bamboos [9].

The vast forest masses of bamboo used commercially for bioenergy are located in the states of Maranhão, Piauí, Pernambuco, Paraíba, and Bahia [10]. Bamboo is regarded as a rapidly growing plant capable of maturing within three to four years, with growth rates ranging from 30 to 100 cm per day, depending on the species. It exhibits a high carbon absorption rate compared with wood. These characteristics enhance its potential as an alternative biomass resource [11].

Brazil has approximately 1.5 million hectares of planted and native bamboo, with an annual production of roughly 150 thousand tons cultivated across all regions. The average yield is 25 tons per hectare, with the state of Acre leading as the main producer. Maranhão focuses its production on biomass for energy generation for the industrial sector, while Paraíba and Pernambuco direct their output to pulp and paper production. States such as São Paulo, Rio Grande do Sul, Minas Gerais, Bahia, and Paraná invest in commercial cultivation aimed at producing panels, edible shoots, and phytocosmetics [12,13].

Bamboo is considered a promising alternative for diversifying the energy matrix, complementing traditional biomass sources such as eucalyptus and pine [14]. Its species are particularly attractive for bioenergy production due to their high productivity, elevated fiber and lignin content, and calorific value [15]. Furthermore, bamboo has a wide range of applications, especially in Asia and Latin America, where it is utilized as an energy source, construction material, panels, pulp, and other products [16].

In the bioenergy context, bamboo plays a relevant role in the implementation of biomass solutions, including solid, liquid, and gaseous fuels. Within biorefineries aimed at maximizing biomass utilization, bamboo has been extensively studied [17,18]. Bamboo-derived biomass and residues exhibit potential for energy utilization and chemical valorization through various thermochemical and biochemical processes [19]. Bamboo possesses suitable characteristics for energy applications, with potential use in various industrial sectors, either as raw biomass or in the production of briquettes, pellets, and charcoal [15,20,21]. However, attention must be paid to ash content, as it may cause boiler-related issues [22].

The yield and chemical properties of pyrolysis products are influenced by operational conditions such as temperature, heating rate, residence times, particle size, and feedstock [23]. Pyrolysis temperatures significantly affect the combustion characteristics of bamboo biochar. The literature reports that increasing temperatures reduce the content of carbon, sulfur, oxygen, hydrogen, volatiles, H/C and O/C ratios, energy yield, heat release rate, and calorific value. Typically, higher temperatures result in improved combustion properties of charcoal with a higher calorific value, reduced volatiles, and lower yields [24,25]. However, elevated pyrolysis temperatures lead to increased energy consumption during the pyrolysis process. Thus, pyrolysis temperature plays a crucial role in the design and optimization of biochar production for commercial development [24].

The choice of specific carbonization parameters depends on a combination of these factors, as well as the specific requirements of the carbonization process in question.

Calorific value refers to the amount of heat generated during the combustion of a unit volume of gas [26]. It serves as an excellent parameter for evaluating the energy potential of biomass fuels [27]. The gravimetric yield of charcoal derived from bamboo species is higher than that of eucalyptus wood at similar carbonization temperatures. Rusch, de Abreu Neto, de Moraes Lúcio and Hillig (2021) reported gravimetric yield values ranging from 34 to 36.9% for bamboo charred at temperatures between 450 and 550 °C [21].

The physical and mechanical properties of bamboo vary according to its anatomical structure, chemical composition, species, and position within the culm [9]. Although classified as simple, the anatomical structure of bamboo culms differs among species, suggesting specific applications for each [28]. Additionally, these variations are influenced by factors such as age, sample position, edaphic characteristics, and climatic conditions [29].

Despite the recognized potential of bamboo for bioenergy and biochar, a significant knowledge gap remains regarding how radial variability (from periphery to interior of the culm wall) in anatomical, chemical, and physical properties affects the suitability of different bamboo species for biochar production. Most studies have focused on a single species or bulk properties, without integrating radial heterogeneity into feedstock selection for pyrolysis. Therefore, the central hypothesis of this study is that the radial position within the bamboo culm wall induces systematic variations in fiber morphology, lignin content, and basic density, which directly influence biochar yield, thermal stability, and pore structure, and that these variations are species-dependent. The novelty of this work lies in (i) the comparative, multi-species assessment of radial gradients (periphery, center, interior) in four bamboo species (*Guadua chacoensis*, *Dendrocalamus strictus*, *Bambusa nutans*, and *Dendrocalamus asper*); (ii) the integration of detailed anatomical characterization, chemical profiling (including S/G lignin ratio), principal component analysis (PCA), and biochar performance evaluation to identify the most suitable species and radial fraction; and (iii) the first techno-economic assessment (TEA) for bamboo-derived biochar based on radial-specific properties, providing a practical framework for sustainable agro-industrial applications. To address these gaps and test our hypothesis, this research investigated the radial anatomical and chemical variations in the culm walls of the four species, linking them to biochar production potential and economic feasibility.

2. Materials and Methods

2.1. Materials

For this study, bamboo samples from four species were utilized: *Guadua chacoensis (Rojas) Londono*, *Dendrocalamus strictus (RoxBambusa) Nees*, *Bambusa nutans Wall. ex Munro*, *and Dendrocalamus asper (Schult. & Schult.f.) Backer* (Table S1, Supplementary Materials). All bamboo samples were collected from culms aged 3–4 years, corresponding to the maturation stage suitable for bioenergy applications based on previous studies. For each species, three healthy clumps (biological replicates) were selected from the same cultivation area in São João do Oeste-PR, except for *Dendrocalamus asper*, which was collected from three clumps in the Silviculture sector of the Federal University of Viçosa (Viçosa, MG, Brazil). Clumps were separated by a minimum distance of 10 m to ensure genetic independence. It is important to note that *Dendrocalamus asper* was collected from a different geographic location (Viçosa, MG, Brazil) compared with the other three species (São João do Oeste, PR, Brazil). Soil and climatic conditions may influence the anatomical, chemical, and physical properties of bamboo. Therefore, direct comparisons among species should consider this limitation, and the observed differences may partially reflect site-specific environmental effects rather than solely genetic or species-level characteristics.

2.2. Sample Preparation

Sampling design: From each of the three clumps (biological replicates) per species, five mature culms (aged 3–4 years) were randomly selected, totaling 15 culms per species. Culms were harvested at ground level, and only internodes free from visible defects or damage were used.

Height standardization: To minimize axial variability, samples were collected exclusively from the third to the sixth internode above ground level (basal to mid-culm position), corresponding to approximately 1.5 to 3.0 m height, depending on the species. This region was chosen because it represents the commercially relevant portion of the culm and exhibits lower axial variation compared with apical or basal extremes.

Radial sampling: From each internode, the culm wall was divided into three radial positions: periphery (outer 5 mm adjacent to the epidermis), center (middle third of wall thickness), and interior (inner 5 mm adjacent to the medullary cavity). For each radial position, samples were pooled across the five culms per clump to obtain one composite sample per biological replicate per radial position, resulting in $n = 3$ biological replicates per species per radial position.

Sample processing: A portion of the chips from each radial position was milled to pass through a 60-mesh sieve for chemical characterization. Another portion was used for basic density determination and anatomical analyses, as described below. Subsequently, samples were separated for histological sectioning, as well as chips from the periphery, center, and interior of the culm walls, aiming at a radial study of the anatomical parameters and basic density. Following the radial sampling, part of the chips was processed into sawdust for chemical characterization, as illustrated in Figure 1.

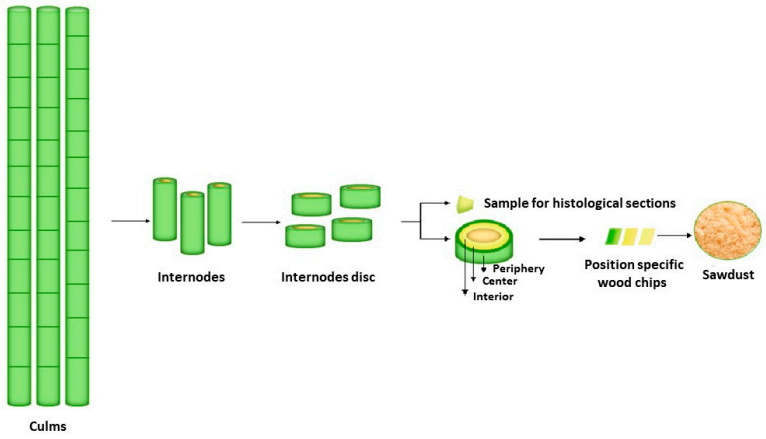

Figure 1. Process for sampling bamboo culms (source: author's own work).

2.3. Bamboo Properties

For the density analysis, chips from the periphery, center, and interior were selected. The determination of basic density was performed using the water immersion method, in accordance with the ABNT NBR 11941 standard.

A suspension of the material was prepared, where the fibers were individualized using hydrogen peroxide and glacial acetic acid, according to the method adapted. The morphological characteristics of the fibers were analyzed using the VALMET FS5 ANALYZER (Valmet Oy, Espoo, Finland), obtaining parameters such as fiber length, width, and wall thickness.

Transverse sections of the test specimens were prepared for microscopic analysis. The samples, with approximate dimensions of 2.0 × 2.0 × 1.0 cm (length, width, and thickness), were subjected to histological sectioning. Photographs were then taken using a camera attached to an optical microscope equipped with a micrometric eyepiece. The AxioVision

image analysis software ((Carl Zeiss Microscopy GmbH, Jena, Germany)) was employed to measure vascular frequency (n mm^{-2}), vessel diameter (μm), parenchyma (%), fibers (%), and vessels (%). The description included the following characteristics: parenchyma and vascular bundles. For the culm wall, which spans from the epidermis to the medullary ring, the description and measurements of anatomical elements were performed based on radial positions: periphery, center, and interior [30,31].

For the elemental analysis of the bamboo samples, the CHNS-O LECO model equipment was used (LECO Corporation, St. Joseph, MI, USA). The percentages of carbon, hydrogen, nitrogen, and sulfur were determined using the TruSpec CHNS Micro module, while oxygen content was calculated by difference.

To determine the structural chemical composition of the bamboo samples, the ground fraction retained on a 60-mesh sieve was used. The determination of the oven-dry content of the samples was performed according to the TAPPI 264 om-88 standard [32].

Extractive content was determined following the TAPPI 204 om-88 standard [33], using the total extractive determination method, substituting ethanol/benzene with ethanol/toluene.

Insoluble and soluble lignin contents were determined in accordance with the TAPPI T222 om-97 and TAPPI um-250 standards. Sugars (glucose, xylose, mannose, galactose, and arabinose) were determined according to the SCAN-CM 71:09 standard [34].

Ash content was determined following the TAPPI T211 om-97 standard [35]. Subsequently, acid digestion of the ash was carried out to determine the concentration of metals (Ca, Mg, Mn, Fe, Cu) using an atomic absorption spectrophotometer. Metal concentrations were assessed based on the TAPPI 266 om-94 standard [36]. Silica content was determined following the TAPPI 244 om-11 standard.

For pyrolysis coupled with gas chromatography and mass spectrometry (Py-GC/MS), bamboo sawdust samples (0.1 mg) were used to calculate the S/G ratio of lignin. Pyrolysis was performed using a microfurnace pyrolyzer (Frontier Laboratories Ltd., Fukushima, Japan) at 550 °C with a residence time of 0.1 min, connected to a GC-MS instrument (QP2020 model Shimadzu Corporation, Kyoto, Japan), employing an Ultra-ALLOY® capillary column (UA5, 30 m × 0.25 mm internal diameter, 0.25 μm film thickness) also supplied by Frontier Laboratories Ltd., Fukushima, Japan [37].

The pyrolysis chamber was purged with helium (100 kPa) to rapidly transfer pyrolysis products to the GC column. The injector temperature was set to 100 °C, and the chromatograph oven temperature was ramped from 45 °C (4 min) to 240 °C at a rate of 4 °C min^{-1}, with the final temperature held for 10 min. The detector and GC-MS interface temperatures were set at 250 °C and 290 °C, respectively.

A mass spectrometer operated in electron-impact ionization mode at 70 eV, with a mass scan range of 50 to 350. The released compounds were identified by comparing their mass spectra with the GC-MS spectral library (Willey and NIST), literature data, and mass fragmentography when necessary. Sixty peaks with the largest areas were measured in duplicate, and the average was reported.

The S/G ratio of lignin was calculated by dividing the sum of the area percentages of syringyl-type lignin (S) by the sum of the area percentages of guaiacyl-type lignin (G) [38,39].

2.4. Statistical Analysis

The experimental design consisted of a 4 × 3 factorial arrangement (four species × three radial positions) with three biological replicates (clumps) per species. Each biological replicate comprised five pooled culms, as described in Section 2.2. The assumptions of normality (Lilliefors test) and homoscedasticity (Cochran test) were verified prior to

ANOVA. The data were subjected to Lilliefors and Cochran tests to assess normality and homogeneity of variance, respectively. Once the assumptions were met, the data were analyzed using analysis of variance (ANOVA), and when significance was established, Tukey's test at a 5% significance level was applied. All analyses were performed using the open-source software R.

Subsequently, a principal component analysis (PCA) was conducted to reduce data dimensionality, grouping them based on similarity and explaining the variance and covariance of the random vectors composed of linear combinations of the original variables. The calculation of the principal components was performed using a PCA algorithm with the aid of the R software version 3.4.3.

2.5. Production and Characterization of Biochar

The production and characterization of biochar were conducted using the bamboo species with the highest potential, selected based on its chemical and structural properties. The pyrolysis process was carried out under controlled conditions to maximize biochar yield and its desirable characteristics, such as high fixed carbon content and low volatile presence [40]. The characterization included physical, chemical, and thermal analyses, evaluating parameters such as porosity, elemental composition, ash content, and thermal stability.

The production of biochar was conducted using *Dendrocalamus strictus* as the selected feedstock. Prior to pyrolysis, the bamboo samples were oven-dried at 103 ± 2 °C until constant mass. The dried material was ground and sieved to obtain a particle size of 2.0–4.0 mm. A sample mass of 10.0 g was placed in a stainless steel fixed-bed reactor (25 mm internal diameter, 300 mm length). The reactor was sealed and purged with nitrogen gas at a flow rate of 100 mL min^{-1} for 15 min. Pyrolysis was performed at atmospheric pressure (101.3 kPa) using a tubular furnace with a programmable temperature controller. The heating rate was set to 10 °C min^{-1} until reaching a final pyrolysis temperature of 550 °C. The sample was held at this temperature for a residence time of 60 min. After the isothermal stage, the reactor was allowed to cool passively to room temperature under a continuous nitrogen flow of 50 mL min^{-1}. The entire experiment was performed in triplicate (n = 3).

2.6. Technical–Economic Assessment (TEA)

A technical–economic assessment of the production of biochar from bamboo residues is necessary to establish its viability on a commercial scale [41,42]. The TEA was conducted based on a detailed analysis of the key parameters involved in biochar production. First, the annual biochar yield per hectare was calculated, considering a 3-year rotation cycle for biomass harvesting. The basic density of the species was used to estimate the amount of available material per unit area. The biochar yield was set at 30%, determining the final product quantity obtained from the processed biomass. The revenue per ton of biochar was established based on a unified market price of US$ 120/ton for agricultural-grade biochar (2024 Brazilian reference). Operational costs were estimated at US$ 31.14/ton of biochar, including harvesting, transport, grinding, pyrolysis (electricity and N_2), labor, and equipment depreciation, based on previous studies [41,42]. It is important to note that this techno-economic assessment is presented as a preliminary estimate. The analysis does not include uncertainty quantification or sensitivity analysis (e.g., variations in biochar price, yield, or transportation costs), as such a detailed assessment is beyond the scope of this study. A full sensitivity analysis is suggested for future work when commercial-scale data become available.

Profit per ton and per hectare was calculated by subtracting production costs from the generated revenue, providing an economic analysis of the feasibility of biochar production from this species. The methodology also accounted for the impact of economic variables, such as transportation, storage, and other indirect costs, which could influence the financial performance of the operation.

3. Results and Discussion

3.1. Characterization and Anatomical Description

The four bamboo species evaluated in this study were not collected from identical sites. While *Guadua chacoensis*, *Dendrocalamus strictus*, and *Bambusa nutans* originated from São João do Oeste-PR, *Dendrocalamus asper* was sampled from Viçosa-MG. Although all plants were mature and apparently healthy, differences in soil type, nutrient availability, climate (temperature, precipitation), and management practices between these two Brazilian regions could contribute to the observed inter-species variability. As such, the results presented here should be interpreted with caution when attributing differences exclusively to species identity. Future studies should aim to collect multiple species from the same provenance or employ common garden experiments to isolate genetic from environmental effects.

Liese (2015) described four basic types of vascular bundles in different bamboo species: Types I, II, III, and IV [28]. Type I is typically found in monopodial bamboo species, while the others are present in sympodial species. Type II features an enlarged fiber sheath on the phloem side, Type III consists of isolated fiber bundles, and Type IV contains a central vascular strand with small sclerenchyma sheaths and two isolated fiber strands located on the sides of the phloem and protoxylem. Fibrovascular bundles exhibit anatomical differences that vary in shape, quantity, and size. These differences can be influenced by the internode height, wall thickness, and position within the culm wall (Figure S1, Supplementary Materials). Below is the anatomical description of each bamboo species studied in this research.

3.1.1. *Dendrocalamus strictus*

The species *Dendrocalamus strictus* features fibrovascular bundles of Type III, where vascular elements are surrounded by a fiber sheath, exhibiting isolated fiber bundles (Figure 2). Dendrocalamus strictus is typically a bamboo species with solid culms, lacking an internal cavity. Its vascular bundles are visible under a ten-fold magnification lens and are distributed throughout the culm, being more numerous near the epidermis (peripheral region, Figure S2, Supplementary Materials).

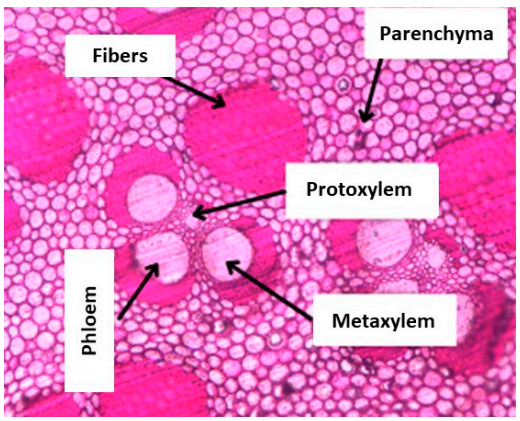

Figure 2. Vascular bundle, fibers, and parenchyma cells of *Dendrocalamus strictus* (source: author's own work).

Regarding the percentage of parenchyma in the species *Dendrocalamus strictus*, this tissue accounts for 74% of the culm composition. The proportions of fibers and vessels observed for the species were 23% and 3%, respectively (Figure 3). In general, the percentage distribution of the wood elements in bamboo species (parenchyma, fibers, and conducting cells) follows a defined pattern. Fibers are concentrated closer to the bark, in the peripheral position, ensuring the material's resistance to wind loads, which are among the most consistent stresses experienced by these species in nature [43].

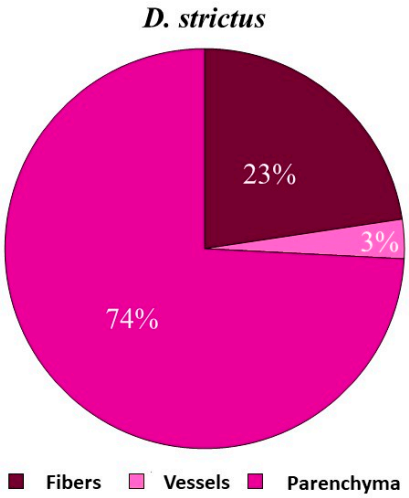

Figure 3. Proportion of anatomical elements in *Dendrocalamus strictus* (source: author's own work).

In Table 1, the vessel diameters (μm) of metaxylem, protoxylem, and phloem in *Dendrocalamus strictus* are shown as a function of the radial position in the culm wall. According to the analysis of variance, the radial position significantly influenced the average vessel diameters.

Table 1. Vessel Diameters (μm) for Metaxylem, Protoxylem, and Phloem.

Radial Position of Bamboo Culm	Metaxylem	Protoxylem	Phloem
Periphery	108.73 a	84.45 b	104.46 b
Center	110.27 a	87.13 a	107.20 a
Interior	101.93 b	83.05 b	94.74 c

Means followed by the same lowercase letters in the columns do not differ statistically, according to Tukey's test at a 95% probability level.

Evaluating the average vessel diameter of the protoxylem reveals that the central position exhibits the highest value for this variable. It was observed that the vessel diameters of the metaxylem and phloem in the inner culm position were significantly smaller than those in other evaluated positions. Indeed, the size in the inner region is smaller due to the reduced quantity of fibers. Sola, da Costa, and de Alcantara (2023) [43] noted that the diameter in the central culm region was statistically similar to that of the periphery but different from the interior. This same pattern was observed in the present study.

The average frequency of vascular elements was 2.2, 2.1, and 1.8 vessels mm^{-2} in the periphery, center, and interior, respectively, with no significant differences among them at a 95% probability level (Figure S3, Supplementary Materials). The frequency of fibrovascular bundles significantly affects the tensile strength of bamboo, as vascular bundles contribute most to its mechanical resistance [44].

3.1.2. *Dendrocalamus asper*

The species *Dendrocalamus asper* features Type III vascular elements surrounded by fiber bundles, but it does not exhibit isolated fiber bundles (Figure 4).

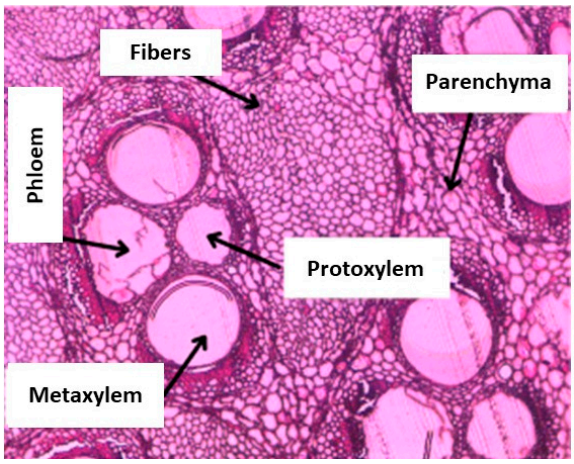

Figure 4. Vascular bundle, fibers, and parenchyma cells of *Dendrocalamus asper* (source: author's own work).

Regarding the percentage of fibers, this tissue accounts for 49% of the culm composition for this species. The proportion of observed parenchyma was 36%, and vessels made up 15%, respectively (Figure 5).

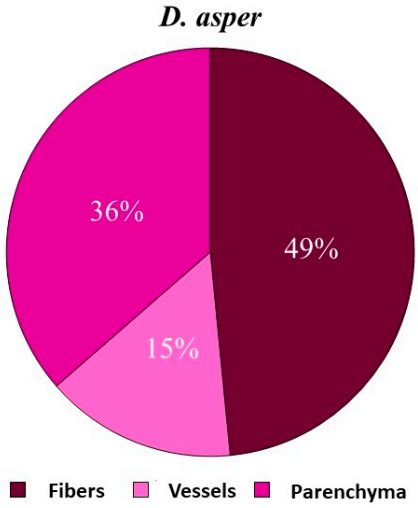

Figure 5. Proportion of anatomical elements in *Dendrocalamus asper* (source: author's own work).

Table 2 presents the vessel diameter values of *Dendrocalamus asper* based on the radial position of the culm wall. According to the analysis of variance, the radial position significantly influenced the average vessel diameter.

Table 2. Vessel Diameters (μm) for Metaxylem, Protoxylem, and Phloem.

Radial Position of Bamboo Culm	Metaxylem	Protoxylem	Phloem
Periphery	193.98 a	128.69 a	223.77 a
Center	192.69 a	127.03 b	212.53 c
Interior	194.08 a	116.04 c	216.69 b

Means followed by the same lowercase letters in the columns do not differ statistically, according to Tukey's test at a 95% probability level.

It can be observed that the vessel diameters of the metaxylem were statistically equal across the three evaluated positions. However, the diameters of the protoxylem and phloem vessels showed variations among the positions. The periphery exhibited larger phloem vessel diameters; in environments where water and nutrients may be scarce, having larger phloem vessels can be an adaptive advantage, enabling more efficient nutrient transport [45].

The vessels in this bamboo species are more numerous near the epidermis (periphery) and gradually decrease toward the interior. The average frequency of vascular elements was 1.5, 1.5, and 1.4 vessels mm^{-2} in the periphery, center, and interior, respectively (Figure S4, Supplementary Materials). The diameter and quantity of vessels influence water and nutrient transport, as well as biomass utilization processes. According to literature, the efficiency of water transport in plants is directly related to the size and frequency of conducting vessels [46]. Furthermore, discuss how these vascular characteristics impact drying and preservation [45].

3.1.3. *Guadua chacoensis*

The species *Guadua chacoensis* features Type III vascular bundles; however, in the peripheral region, all vascular elements are encompassed by fiber sheaths and exhibit a small quantity of parenchyma cells (Figure 6).

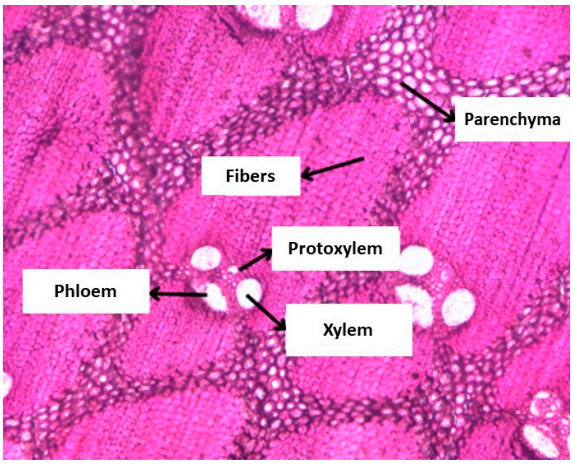

Figure 6. Vascular bundle, fibers, and parenchyma cells of *Guadua chacoensis* (source: author's own work).

Regarding the percentage of fibers, this tissue accounts for 52% of the culm composition (Figure 7). The observed proportions of parenchyma and vessels for the species were 40% and 8%, respectively.

Table 3 presents the vessel diameter values of *Guadua chacoensis* based on the radial position of the culm wall. According to the analysis of variance, the radial position significantly influenced the average vessel diameter.

Table 3. Vessel Diameters (μm) for Metaxylem, Protoxylem, and Phloem.

Radial Position of Bamboo Culm	Metaxylem	Protoxylem	Phloem
Periphery	89.08 c	54.93 c	139.71 c
Center	152.27 a	87.52 a	205.71 a
Interior	141.44 b	85.93 b	142.95 b

Means followed by the same lowercase letters in the columns do not differ statistically, according to Tukey's test at a 95% probability level.

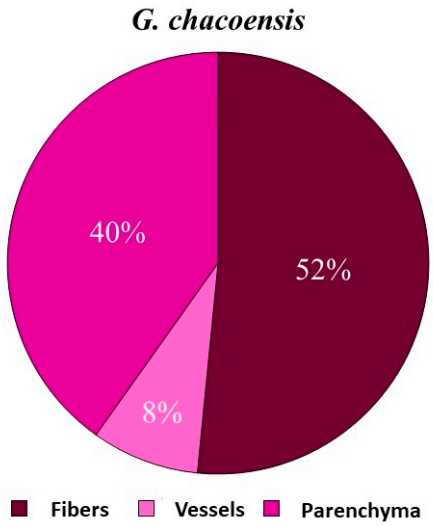

Figure 7. Proportion of anatomical elements in *Guadua chacoensis* (source: author's own work).

The vessel diameters of the metaxylem, protoxylem, and phloem in the periphery of the culm were significantly smaller than in the other evaluated positions. The metaxylem exhibits a larger diameter compared with the protoxylem. From an engineering perspective, it is essential to understand the vessel diameters and distribution along the wall thickness [42].

The vascular bundles of bamboo, visible under a ten-fold magnification lens, are more numerous near the epidermis. These vessels have smaller diameters in the peripheral region, gradually increasing toward the interior. The average frequency of vascular elements was 2.2, 1.7, and 1.5 vessels mm^{-2} in the periphery, center, and interior, respectively (Figure S5, Supplementary Materials).

3.1.4. *Bambusa nutans*

The species *Bambusa nutans* features Type III vascular bundles, with all vessels encompassed by fiber sheaths (Figure 8). Regarding the percentage of fibers, this tissue accounts for 51% of the culm composition (Figure 9). The observed proportions of parenchyma and vessels for the species were 42% and 7%, respectively. Table 4 presents the vessel diameter values of *Bambusa nutans* based on the radial position of the culm wall. According to the analysis of variance, the radial position significantly influenced the average vessel diameter.

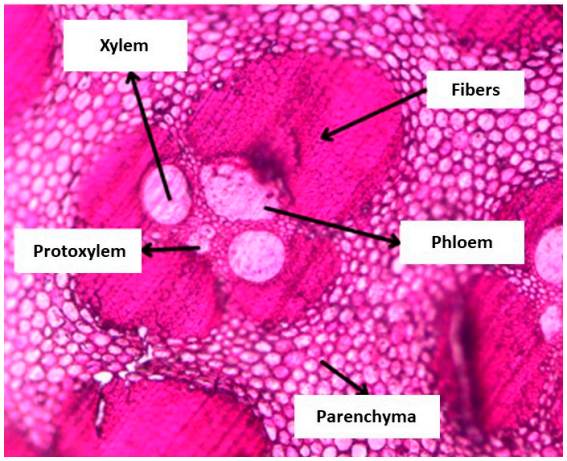

Figure 8. Vascular bundle, fibers, and parenchyma cells of *Bambusa nutans* (source: author's own work).

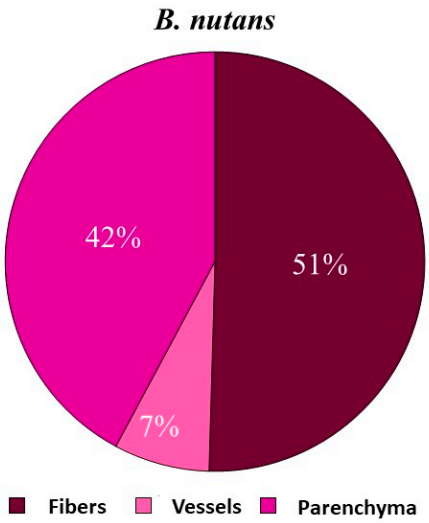

Figure 9. Proportion of anatomical elements in *Bambusa nutans* (source: author's own work).

Table 4. Vessel Diameters (μm) for Metaxylem, Protoxylem, and Phloem.

Radial Position of Bamboo Culm	Metaxylem	Protoxylem	Phloem
Periphery	82.52 c	38.14 c	113.73 c
Center	156.33 b	87.76 b	203.26 b
Interior	175.97 a	92.09 a	211.12 a

Means followed by the same lowercase letters in the columns do not differ statistically, according to Tukey's test at a 95% probability level.

The largest vessel diameters were observed in the interior of the culm wall, with a reduction in diameter as it approaches the periphery. The sizes of the metaxylem, protoxylem, and phloem vessels were 53.1%, 58.5%, and 46.1% larger in the interior region compared with the periphery. Sola, da Costa, and de Alcantara (2023) reported that the sizes of metaxylem and phloem vessels were 28.4% and 33.3% larger in the interior region relative to the periphery [43]. This pattern aligns with the findings of Grosser and Liese (1971) [47], where larger-diameter vessels were observed in the internal regions and smaller ones in the periphery. The peripheral zone is composed of vascular bundles adjacent to the epidermis, which are smaller, more numerous, and contain fewer parenchyma cells between them. The average frequency of vascular elements was 2.1, 1.3, and 0.9 vessels mm^{-2} in the periphery, center, and interior, respectively (Figure S6, Supplementary Materials).

3.2. Effect of Radial Position on Anatomical Elements Based on Bamboo Species

3.2.1. Vessels

According to the analysis of variance, there was an interaction effect between species and radial position in the culm on the proportion of vessels. Table 5 presents the mean values of the proportion of vessels in bamboo based on radial position and species. The highest values were observed for *Dendrocalamus asper* and the lowest for *Dendrocalamus strictus*. Regarding the evaluated radial positions, it can be noted that the periphery and center showed similar values for *Dendrocalamus strictus* and *Dendrocalamus asper*. Meanwhile, Guadua chacoensis and Bambusa nutans presented similar values only for the center and interior of the culm wall, these being the highest among the positions. As for the shape of the vascular bundle in the peripheral region, the fiber sheaths are more compact, reducing intercellular space and influencing the proportion of vessels [48].

Table 5. Proportion of Vessels (%) in the Four Bamboo Species.

Radial Position in the Culm	*D. strictus*	*D. asper*	*G. chacoensis*	*B. nutans*
Periphery	3.99 ac	15.13 aba	5.97 ab	4.7 abc
Center	4.33 ac	16.65 aa	9.19 ab	8.38 ab
Interior	1.18 ac	13.7 aa	9.67 ab	9.05 ab

Means followed by the same lowercase letters in the columns do not differ statistically, according to Tukey's test at a 95% probability level.

3.2.2. Parenchyma

According to the analysis of variance, there was no interaction effect between species and radial position in the culm for parenchyma percentages; only isolated effects were observed. Table 6 presents the mean values of the proportion of parenchyma based on the radial position of the culm wall.

Table 6. Mean Values of Parenchyma Based on Radial Position.

Radial Position of the Culm	Mean Values (%)
Periphery	40.86 c
Center	44.99 b
Interior	58.81 a

Means followed by the same lowercase letters in the columns do not differ statistically, according to Tukey's test at a 95% probability level.

Regarding the proportion of parenchyma cells, the interior of the culm exhibited higher mean values, meaning parenchyma is more abundant in the inner layers of the culm and decreases as it approaches the periphery. This behavior is associated with the increase in fiber proportion closer to the peripheral region of the culm wall. Table 7 presents the mean values of the proportion of parenchyma based on the bamboo species.

Table 7. Mean Values of Parenchyma Based on Bamboo Species.

Species	Mean Values (%)
Bambusa nutans	42.17 b
Dendrocalamus strictus	74.19 a
Dendrocalamus asper	36.39 c
Guadua chacoensis	40.15 bc

Means followed by the same lowercase letters in the columns do not differ statistically, according to Tukey's test at a 95% probability level.

Dendrocalamus strictus exhibited the highest proportion of parenchyma cells. Across all species, this tissue was more abundant in the inner layers of the culm and decreased toward the outermost layer. Regarding parenchyma percentage, Brito et al. (2015) [49] observed that this tissue occupies 50.72% of the culm composition in *Dendrocalamus giganteus*. These authors reported that the proportion of parenchyma was more abundant in the inner layers of the culm, decreasing toward the outer layer.

3.2.3. Fibers

Percentage of Fibers

According to the analysis of variance, there was no interaction effect between species and radial position in the culm for fiber percentages; only isolated effects of the variables were observed. Table S2 (Supplementary Materials) presents the values of fiber proportions based on the radial position of the culm wall. Analyzing the simple effects of the positions, the periphery exhibited the highest proportion of fibers. Ghavami, Perazzo Barbosa, and

Eustáquio Moreira (2017) observed an increase in fiber proportions radially from the interior to the outer face, allowing bamboo to withstand wind loads [42].

Table S3 (Supplementary Materials) displays the fiber proportion values across species. Among the species, the fiber proportion values were statistically similar for *Guadua chacoensis*, *Bambusa nutans*, and *Dendrocalamus asper*. *Dendrocalamus strictus* showed the lowest fiber proportion, which may be linked to its higher proportion of parenchyma. Fibers are associated with vascular bundles, either as sheaths or isolated fibers, and constitute 40–50% of the culm's mass [50].

For the proper utilization of fibers, understanding their structural modifications and dimensional characteristics within the culm wall is essential. The dimensions of fibers help define specific properties and applications for each studied material. According to the analysis of variance, an interaction was observed between species and radial positions for the morphological parameters shown in Table 8.

Table 8. Mean Values of Bamboo Fiber Morphology.

Property	Radial Position	Species			
		D. strictus	*D. asper*	*G. chacoensis*	*B. nutans*
Length (mm)	Periphery	1.80 ab	1.91 aa	1.76 ac	1.80 bb
	Center	1.79 ab	1.73 bc	1.65 bd	1.86 aa
	Interior	1.67 ba	1.63 cb	1.40 cd	1.53 cc
Width (μm)	Periphery	18.72 bc	18.34 bd	19.75 ba	19.14 cb
	Center	19.07 ac	21.36 aa	21.32 aa	21.02 ab
	Interior	18.70 bc	21.14 aa	19.87 bb	20.16 bb
Wall Thickness (μm)	Periphery	5.56 ac	4.53 ad	7.11 aa	6.13 bb
	Center	5.42 ac	3.15 bd	6.31 bb	6.74 aa
	Interior	4.79 bc	2.21 cd	5.45 cb	5.95 ba

Means followed by the same lowercase letters in the columns do not differ statistically, according to Tukey's test at a 95% probability level.

The species *Dendrocalamus asper*, *Dendrocalamus strictus*, *Bambusa nutans*, and *Guadua chacoensis* exhibited average fiber lengths of 1.75 mm, 1.75 mm, 1.73 mm, and 1.60 mm, respectively. Liese (2002) established a relationship between fiber length and internode length, indicating that species with longer fibers also tend to have longer internodes [51]. The longest fiber lengths observed were for *Dendrocalamus asper* at the periphery, *Bambusa nutans* at the center, and *Dendrocalamus strictus* in the interior. Radial position analysis showed that the longest fibers were generally found at the periphery for all species, except for *Bambusa nutans*, where the longest fibers were observed at the center.

Species with wider fibers included *Dendrocalamus asper*, *Guadua chacoensis*, and *Bambusa nutans*. These species exhibited a consistent radial position pattern, where the widest fibers were found in the central region, followed by the inner culm area. Fiber wall thickness ranged from 2.21 to 7.11 μm, and classified fibers within this thickness range as thick-walled [52]. The highest wall thickness values were observed for *Guadua chacoensis* and *Bambusa nutans*, while *Dendrocalamus asper* exhibited the lowest values.

Wall thickness and fiber length are key parameters associated with fiber resistance, impacting properties like density and dimensional stability [53]. The study confirmed this correlation, showing that species with lower density possessed thinner-walled fibers. Radial analysis revealed that the highest wall thickness values occurred at the periphery, except for Bambusa nutans, where the central region showed greater wall thickness.

According to the International Association of Wood Anatomists (IAWA), fibers are categorized into three groups: medium length (0.91–1.60 mm), moderately long (1.61–2.20 mm), and very long (2.21–3.00 mm). The studied species exhibited fiber lengths ranging from 1.61 to 1.77 mm, classifying them as moderately long fibers.

3.3. Basic Density

Basic density is a key quality property of lignocellulosic materials, as it correlates with the chemical, physical, and anatomical properties of biomass. The average values of basic density for each bamboo species, considering the positions, can be observed in Table 9.

Table 9. Mean Values of Basic Density (kg/m^3) of Bamboo Based on Culm Wall Positions.

Position	Species			
	D. strictus	***D. asper***	***G. chacoensis***	***B. nutans***
Periphery	569 ab	354 ac	835 aa	858 aa
Center	549 ab	151 bc	545 bb	712 ba
Interior	432 ba	145 bb	359 ca	479 ca

Means followed by the same lowercase letters in the columns do not differ statistically, according to Tukey's test at a 95% probability level.

The analysis of variance indicated a significant interaction between species and culm position for basic density. *Bambusa nutans* showed the highest density values across all culm positions, as well as the highest mean density for the species, followed by *Guadua chacoensis*. Conversely, *Dendrocalamus asper* had the lowest density values, both across positions and the mean. In all studied species, the highest basic density was found at the periphery of the culms. The differences in density between peripheral and internal regions of the culms can be exploited for separation in physical processing. This variation in basic density within the culm wall is due to the predominance of fibrous tissue in the outer region and parenchymatous tissue in the inner regions.

The results revealed an increase in density values from the inner region to the peripheral region of the culm. This behavior is associated with the heterogeneity of bamboo, as its vascular bundle distribution is non-uniform, leading to reduced density and challenges in product stability, causing variability in shrinkage and swelling properties [24].

The observed mean values were 516, 216, 579, and 683 kg/m^3 for Dendrocalamus strictus, *Dendrocalamus asper*, *Guadua chacoensis*, and *Bambusa nutans*, respectively. For *Bambusa nutans*, the literature reported an average density of 556 kg/m^3, which is lower than the value found in the present study but similar to the value of 615 kg/m^3 reported by Ciaramello and Azzini (1971) for this species at two to three years of age [54]. These authors also noted that among the studied bamboo species, *Bambusa nutans* was the densest, consistent with the findings of the present work.

The average basic density observed for *Guadua chacoensis* aligns with data the literature, who suggested that the basic density of the *Guadua genus* ranges from 450 to 650 kg/m^3. Additionally, Marafon et al. (2019) reported an average density of 577 kg/m^3 for *Guadua angustifolia* [15]. The average basic density values of *Dendrocalamus asper* in the present study were lower than those reported by Siam et al. (2019) [55], who found average values of 559 kg/m^3. Similarly, Santos et al. (2016) reported a value of 604 kg/m^3 for five-year-old *Dendrocalamus asper* [56].

3.4. Chemical Characterization

3.4.1. Elementary Analysis

The analysis of variance demonstrated no significant interaction between the factors for carbon, hydrogen, and oxygen content, with only isolated effects observed for species and culm position (Table 10 and Table S4, Supplementary Materials). According to Tukey's test, the mean carbon contents for the four species are statistically equivalent, as are the values for the three radial positions (Table 10). Carbon content is highly significant for both charcoal production and direct combustion. For hydrogen content, no interaction was observed

between positions and species. Analyzing the simple effects among species, *Dendrocalamus asper* and *Guadua chacoensis* exhibited the highest mean values. Regarding radial positions, hydrogen values were statistically equivalent. During combustion, hydrogen releases more energy than carbon. Despite its lower concentration, hydrogen content is crucial for energy production [57].

Table 10. Mean Values of Carbon, Hydrogen, and Oxygen Content for Bamboo Species.

Property	*D. strictus*	*D. asper*	*G. chacoensis*	*B. nutans*
Carbon (%)	44.73 a	44.92 a	44.33 a	45.10 a
Hydrogen (%)	5.36 b	5.60 a	5.60 a	5.37 b
Oxygen (%)	49.52 a	48.68 a	49.75 a	49.29 a

Means followed by the same lowercase letters in the columns do not differ statistically, according to Tukey's test at a 95% probability level.

For oxygen content, no interaction was observed between radial positions and species. Oxygen contents were statistically equivalent across both species and positions. Oxygen negatively affects calorific value, as compounds with higher oxygen content tend to store less energy [57].

For nitrogen and sulfur contents, the interaction between species and positions was significant. Among the species, *Dendrocalamus asper* exhibited the highest mean nitrogen and sulfur contents, at 0.68% and 0.12%, respectively. Conversely, *Bambusa nutans* presented the lowest nitrogen content, while *Guadua chacoensis* displayed the lowest sulfur content. For *Dendrocalamus strictus*, *Guadua chacoensis*, and *Bambusa nutans*, no statistical differences in nitrogen content were observed across the three radial positions. However, *Dendrocalamus asper* showed higher nitrogen content in the inner region (Table S5, Supplementary Materials). The presence of nitrogen and sulfur in biomass directly impacts environmental pollution, due to the formation of harmful oxides and volatile compounds [58].

Regarding sulfur content, no statistical differences were observed between positions for *Dendrocalamus asper* and *Guadua chacoensis*. For *Dendrocalamus strictus* and *Bambusa nutans*, the highest sulfur content was found at the periphery. Sulfur content in biomass affects fuel quality and has environmental implications, as sulfur oxides (SO_2) released during combustion are atmospheric pollutants [59]. On average, plant biomass has very low sulfur content, ranging from 0.01% to 0.2% on a dry basis [60].

3.4.2. Structural Chemical Analysis

Analyzing the structural chemical composition, an interaction between bamboo species and radial positions was observed in Table 11. Among the species, *Dendrocalamus strictus* exhibited the lowest extractives content (1.53%), while *Bambusa nutans* had the highest (3.52%). Across radial positions, only *Bambusa nutans* showed variations, with the highest extractive content observed in the inner culm wall. Potenciano Marinho et al. (2012) [61] found that bamboo samples at two years of age had the highest extractive contents, both in ethanol-toluene extractives and total extractives. In contrast, bamboo samples at six years of age exhibited the lowest extractive contents, indicating that bamboo age significantly impacts the concentration of extractives, with younger bamboo containing higher levels of these compounds. No numerical relationship between extractive contents and the age of the materials was observed in the present study.

The analysis of variance revealed a significant effect of radial culm positions on lignin content for all species. The highest lignin contents, ranging from 28.0% to 30.40%, were found in the peripheral region, except for *Dendrocalamus asper*, which showed higher lignin content in the inner culm wall. This behavior, according to Rusch et al. (2021) [62], may be linked to bamboo lignification, which occurs from the base to the top of the stem and

from the outer to the inner culm wall, being more intense around the xylem vessels. This could be related to the higher concentration of fiber bundles in the peripheral region and the increase in parenchyma cells in the inner region.

Table 11. Contents of Extractives, Lignin, and Ash (%) in Bamboo Based on Culm Position.

Property	Position	*D. strictus*	*D. asper*	*G. chacoensis*	*B. nutans*
Total Extractives	Periphery	1.46 ac	2.2 ab	2.18 ab	3.17 ba
	Center	1.76 ac	2.46 ab	2.04 abc	3.34 ba
	Interior	1.37 ac	2.13 ab	2.44 ab	4.06 aa
Total Lignin	Periphery	30.40 aa	26.14 bd	28.86 ab	28.0 ac
	Center	29.51 ba	25.28 cd	27.06 bb	26.12 cc
	Interior	29.07 ca	28.27 ac	28.63 ab	26.88 bd
Carbohydrates	Periphery	62.8 cd	68.05 ba	63.8 cc	65.9 cb
	Center	64.5 ad	69.15 aa	67.55 ac	68.5 ab
	Interior	63.85 bd	67.6 ca	64.7 bc	66.8 bb
Ashes	Periphery	2.2 cb	3.2 ca	2.04 cb	1.74 bc
	Center	2.99 bb	3.4 ba	2.48 bc	1.62 bd
	Interior	3.84 aa	3.76 aa	2.84 ab	1.93 ac

Means followed by the same lowercase letters in the columns do not differ statistically, according to Tukey's test at a 95% probability level.

Literature reports lignin contents ranging from 22.63% to 32.65% for bamboo species [61]. High lignin contents can give bamboo excellent physical and mechanical properties [63]. It is worth mentioning that lignin, as the thermally most stable component, can contribute to higher charcoal yields when present in larger amounts. With 60–64% elemental carbon in its molecular composition, lignin is the main constituent responsible for increased calorific value.

Carbohydrate content varied across species and radial positions. *Dendrocalamus asper* and *Bambusa nutans* exhibited the highest mean carbohydrate contents, at 68.27% and 67.07%, respectively. Previous studies found increased carbohydrate content in Bambusa vulgaris with age [22]. All evaluated species showed variations in carbohydrate contents across radial positions, with the highest values found in the central region, followed by the inner region. Studies on three-year-old bamboo species reported carbohydrate contents ranging from 74.62% to 84.53%, with the highest content found in the outer region [64].

Ash contents varied across positions and species. For all species, the highest ash content was found in the inner culm wall. Inorganic substances are predominantly present in the inner layers of the culm. In his study, only silicon was more concentrated in the epidermis [48]. Among the species, mean ash content ranged from 1.76% in *Bambusa nutans* to 3.15% in *Dendrocalamus asper*. Santos (2023) reported an ash content of 2.96% for *Bambusa nutans* [65]. Liese et al. (2015) noted that ash quantity is influenced by bamboo growth locations, and differences among species may be linked to soil and climate in the cultivation areas [28].

3.4.3. Ash Constituents

According to the analysis of variance, the highest values of substances insoluble in hydrochloric acid, including silica, were found in the periphery for all species. However, *Dendrocalamus strictus* exhibited the highest silica content in the inner culm wall (Table 12). Among the evaluated species and radial positions, *Guadua chacoensis* exhibited the highest content of insoluble substances. Silica, considered an impurity, is undesirable in combustion processes. Lower silica content can help minimize erosion and slag formation issues during biomass processing. *Guadua chacoensis* had the highest insoluble content, while *Dendrocalamus asper* presented the lowest. The characteristics of the ash are correlated with

the composition of the raw material. The analysis of variance revealed variations in ash constituents across the studied species and radial positions.

Table 12. Content of Insolubles in HCl (Silica) (%).

Property	Position	Species			
		D. strictus	*D. asper*	*G. chacoensis*	*B. nutans*
Insoluble HCl	Periphery	0.95 cc	1.1 abc	2.0 aa	1.37 ab
	Center	1.5 bb	0.37 cc	2.0 aa	1.20 ab
	Interior	2.0 aa	0.73 bc	2.0 aa	1.29 ab

Means followed by the same lowercase letters in the columns do not differ statistically, according to Tukey's test at a 95% probability level.

The most abundant elements in the bamboo culm biomass ash in this study were manganese (Mn), magnesium (Mg), and calcium (Ca) (Table 13).

Table 13. Mean Values of Bamboo Ash Constituents (mg/Kg).

Property (mg/kg)	Radial Position	Species			
		D. strictus	*D. asper*	*G. chacoensis*	*B. nutans*
Calcium (Ca)	Periphery	10.5 cc	5.7 cd	23.17 ba	18.37 ab
	Center	16.4 ab	13.73 ac	21.57 ca	7.8 bd
	Interior	12.1 bb	10.17 bc	23.5 aa	3.9 cd
Magnesium (Mg)	Periphery	47.37 aa	39.3 ac	19.7 cd	40.97 cb
	Center	41.37 cb	37.27 bc	20.87 bd	46.8 ba
	Interior	43.5 cb	29.5 cc	24.4 ad	53.7 aa
Manganês (Mn)	Periphery	20.57 bd	35.7 bb	41.07 ba	25.5 cc
	Center	31.6 ad	37.8 ab	45 aa	33.97 ac
	Interior	33.5 ac	36.7 abb	42.57 ba	28 bd
Iron (Fe)	Periphery	11.13 ab	12.33 ba	8.5 ac	12.7 aa
	Center	5.93 ca	2.07 cc	6.13 ba	5.47 bb
	Interior	6.4 bb	14.5 aa	3.1 cd	5.13 bc
Copper (Cu)	Periphery	2.87 ab	5.53 ca	0.43 bd	1.30 ac
	Center	2.23 bb	8.07 aa	0.30 bd	1.47 ac
	Interior	2.77 ab	7.17 ba	1.27 ac	1.30 ac

Means followed by the same lowercase letters in the columns do not differ statistically, according to Tukey's test at a 95% probability level.

3.4.4. Syringyl/Guaiacyl Ratio (S/G)

Biomasses with higher syringyl unit content tend to be more thermally stable and exhibit more uniform decomposition, which is advantageous for biochar production [66]. Furthermore, an optimal balance between syringyl (S) and guaiacyl (G) units can enhance the efficiency of biomass conversion into bioenergy due to variations in the reactivity of bonds between the subunits [67]. Therefore, analyzing the S/G ratio enables the optimization of energy conversion processes and charcoal production, making them more efficient and sustainable.

The analysis of variance revealed an interaction between the evaluated species and radial positions. Among the species, *Dendrocalamus strictus* exhibited the lowest S/G ratio. On the other hand, *Bambusa nutans* showed the highest S/G ratio, with the maximum value observed in the inner culm wall (Table 14).

For *Dendrocalamus asper*, the S/G ratio values were similar across the three evaluated radial positions. In contrast, *Guadua chacoensis* exhibited the highest S/G ratio in the inner culm wall. Across all species, the lowest S/G ratio values were found in the peripheral region. *Dendrocalamus strictus* and *Dendrocalamus asper* displayed a similar pattern, with S/G values increasing from the periphery to the center and then decreasing in the inner culm wall. Conversely, for *Guadua chacoensis* and *Bambusa nutans*, the S/G ratio progressively increased from the periphery to the inner culm wall.

Table 14. Syringyl/Guaiacyl (S/G) Ratio of Lignin.

Variable	Position	Species			
		D. strictus	*D. asper*	*G. chacoensis*	*B. nutans*
S/G	Periphery	0.6 bb	1.08 aab	1.27 bab	1.4 ba
	Center	1.32 ab	1.41 ab	1.52 bb	1.8 ba
	Interior	1.04 abb	1.19 ab	2.64 aa	5.12 ab

Means followed by the same lowercase letters in the columns do not differ statistically, according to Tukey's test at a 95% probability level.

Guaiacyl lignin contains more elemental carbon than syringyl in its molecular structure. Ideally, biomasses with lower S/G ratios in lignin should be sought for energy applications [68]. The composition of lignin, particularly the type and proportion of syringyl to guaiacyl units (S/G), has a significant impact on energy production from biomass.

A lower S/G ratio is preferable for lignocellulosic compounds in energy applications, as a lower presence of syringyl units compared with guaiacyl units in lignin structure delays thermal degradation during combustion [22]. Additional studies support this assertion. For instance, Sannigrahi et al. (2010) observed that an excess of syringyl units can hinder combustion efficiency [69]. Similarly, Pu et al. (2013) found that a higher proportion of guaiacyl units can enhance the thermal stability of lignin, making it more suitable for energy generation [70].

3.5. Principal Component Analysis (PCA)

Principal Component Analysis (PCA) was conducted based on the correlation matrix between the anatomical, chemical properties, and basic density of bamboo biomass species. To identify the most significant properties for discriminating bamboo species, the analysis excluded variables associated with the highest eigenvector in the principal component with the lowest eigenvalue [71]. This process was carried out by removing one variable at a time and repeating the procedure after each removal.

According to the criteria adopted in this study, principal components with eigenvalues greater than 1 were selected. As a result, the first two components were extracted, which together explain 85.11% of the total variability in the dataset. Information regarding the correlation between the study variables can be determined using the cosine of the angle formed between two vectors. If both vectors have the same orientation, a positive correlation exists between the variables. Conversely, if the vectors have opposing orientations, a negative correlation is present. However, if two vectors are nearly perpendicular, the correlation approaches zero (Figure 10).

The analysis enabled the selection of eight representative parameters for discriminating the evaluated bamboo species and positions. Basic density and wall thickness showed a positive correlation, with the angle formed between the vectors being close to 0°, indicating that wall thickness significantly contributes to increased basic density. Fibers with high wall thickness values exhibit greater mass to support thermal decomposition, enhancing the yield and quality of biochar [22]. In this study, higher basic densities were associated with species having thicker fiber walls and smaller pore diameters. Thus, fibers with thicker walls are desirable to achieve the highest possible density.

As expected, lignin and carbohydrate contents showed a strong negative correlation, with the vectors forming an angle close to 180°. Given that the cellular wall composition is almost entirely lignin and carbohydrates, there is a marked negative correlation between the two; an increase in lignin content corresponds to a decrease in carbohydrate content [44]. The proportion of fibers and carbohydrates exhibited a positive correlation, with their vectors forming an angle smaller than 90°. Basic density, fiber proportion, and lignin

content also showed a positive correlation, with their vectors forming an angle smaller than 90°.

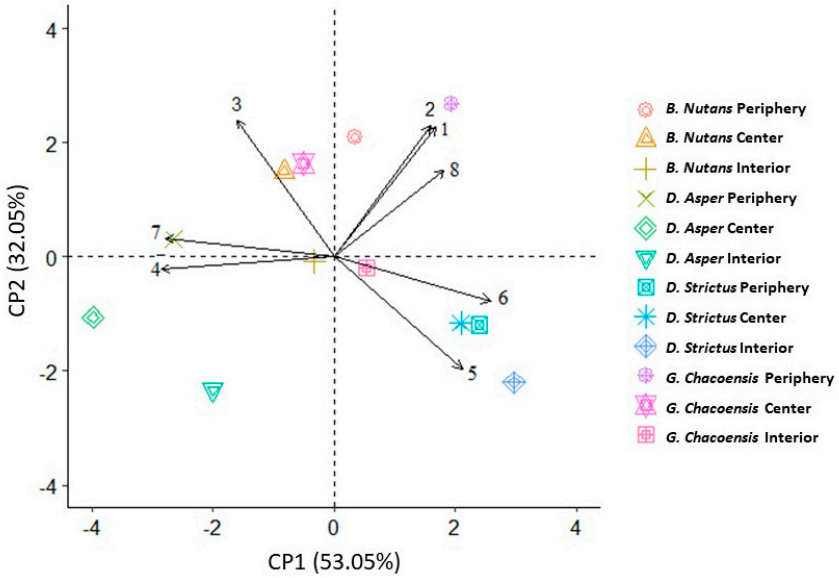

Figure 10. Vectors of bamboo properties and score dispersion in relation to principal components 1 and 2 (Where: Basic Density (1), Wall Thickness (2), Fiber Proportion (3), Parenchyma Proportion (4), Vessel Proportion (5), Lignin Content (6), Carbohydrate Content (7), and Insolubles (8)).

The study of dissimilarity among bamboo species using a graphical biplot representation of the principal components was performed by observing the proximity of points on the plot. Materials farther apart are more dissimilar than those closer together. From the graph, it is apparent that the species *Dendrocalamus asper* is significantly more distant from the others, with only the characteristics of the peripheral region resembling those of *Guadua chacoensis* in the center and *Bambusa nutans*.

3.6. Biochar Production and Characterization

To select the most suitable bamboo species for biochar production, a comparative analysis was performed based on key biomass properties that directly influence biochar yield, thermal stability, and carbon sequestration potential: total lignin content (higher is favorable), syringyl/guaiacyl (S/G) ratio (lower is favorable), elemental carbon content, basic density, and ash content. Table 15 summarizes these parameters for the four species, considering the peripheral region of the culm, which is the most relevant for biochar production due to its higher lignin and fiber content [72–74].

Dendrocalamus strictus exhibited the highest lignin content (30.40%) and the lowest S/G ratio (0.60) among all species. Higher lignin content is known to increase biochar gravimetric yield and thermal stability, while a lower S/G ratio indicates a higher proportion of guaiacyl units, which enhances thermal degradation resistance and carbon retention during pyrolysis [22,69,70]. Although *B. nutans* and *G. chacoensis* showed higher basic density and lower ash content, their higher S/G ratios and lower lignin contents make them less suitable for biochar production when considering long-term carbon sequestration and energy efficiency. *Dendrocalamus asper* presented the lowest lignin content and the lowest basic density, which would likely result in lower biochar yield and poorer mechanical stability [75]. Therefore, *D. strictus* was selected as the most promising feedstock for biochar production. Moreover, its lower carbohydrate proportion (Table 11) further reduces volatile release during pyrolysis, leading to a higher fixed carbon content in the final biochar.

Table 15. Standards for Biochar Characterization.

(a)					
Species	**Lignin (%)**	**S/G Ratio**	**Carbon (%)**	**Basic Density (kg/m^3)**	**Ash (%)**
Dendrocalamus strictus	30.40	0.60	44.73	569	2.20
Dendrocalamus asper	26.14	1.08	44.92	354	3.20
Guadua chacoensis	28.86	1.27	44.33	835	2.04
Bambusa nutans	28.00	1.40	45.10	858	1.74
(b)					
Parameters				**Standard**	
Elemental chemical composition				DIN EN 15104	
Insolubles HCl (Silica)				TAPPI 244 om-11	
Metals				TAPPI 266 om-94	
Higher heating value				ABNT NBR 8633	

The samples of *Dendrocalamus strictus* were dried in an oven at a temperature of 103 ± 2 °C until a constant mass was achieved. The pyrolysis process was conducted under an inert atmosphere using nitrogen as the purge gas to ensure anaerobic conditions and prevent oxidation of the biomass [76,77]. The gravimetric yield (based on dry mass) of biochar was determined according to Equation (1).

$$RG = \frac{MC}{MB} \times 100 \quad (1)$$

where:

RG = Gravimetric yield of biochar (%);

MC = Mass of biochar (g);

MB = Dry mass of bamboo (g).

The fixed carbon (FC) content (%) was indirectly determined as part of the proximate analysis, following the standard procedure outlined in ABNT NBR 8112 (1986). It was calculated by subtracting the total volatile matter (VM) and ash content (A) from 100%, as shown in Equation (2).

$$\text{Fixed Carbon (\%)} = 100 - \text{Volatile Matter (\%)} - \text{Ash Content (\%)} \quad (2)$$

Thermogravimetric analysis (TGA) and X-ray diffraction (XRD) were conducted for the biochar, following the methodology standard [78,79]. The specific surface area of the biochars was obtained using the Brunauer, Emmett, and Teller (BET) equation, developed in 1938, which relates values obtained from adsorption isotherms to the specific area of a solid. The analysis was performed using the AUTOSORB-1 equipment (Quantachrome Instruments, Boynton Beach, FL, USA), with nitrogen gas as the adsorbate at 77 K. Prior to the analysis, approximately 10 mg of each biochar sample was degassed at 150 °C for 4 h under a nitrogen flow to remove any adsorbed impurities. Table 15 presents the standards used for the characterization analyses of the biochar.

The average values of gravimetric yield and the properties of the biochars produced from the different bamboo species are presented in Table 16. It is important to distinguish between elemental carbon (determined by CHNS elemental analysis, representing total carbon atoms in the biochar matrix) and fixed carbon (calculated from proximate analysis, representing the non-volatile carbon fraction that remains after pyrolysis and is thermally stable). For carbon sequestration applications, fixed carbon is the more relevant parameter because it correlates with the biochar's resistance to mineralization in soil. The carbon

sequestration potential can be estimated from the fixed carbon content, assuming that this fraction remains stable under typical soil conditions over decadal to centennial timescales.

Table 16. Average yield values and properties of Biochar from *Dendrocalamus strictus*.

Property	Biochar	Note
Gravimetric Yield (%)	31.14 c	
Carbon (%)	89.66 b	CHNS analysis
Hydrogen (%)	1.31 a	
Nitrogen (%)	0.132 c	
Sulfur (%)	0.031 a	
Oxygen (%)	6.86 c	
Volatile Materials (%)	6.83 c	Proximate Analysis
Ashes (%)	8.20 c	
Fixed Carbon (%)	84.97	Calculated: 100—VM—Ash
HCl Insolubles (Silica (%))	2.83 c	

Means followed by the same lowercase letter do not differ significantly according to Tukey's test ($p < 0.05$). Values are presented as mean ± standard deviation (SD). For results obtained in triplicate, variability between measurements was minimal; thus, standard deviation values are not shown.

The analysis of the average gravimetric yield and properties of *Dendrocalamus strictus* biochar highlights its favorable characteristics for both agricultural and energy applications. A gravimetric yield of 31.14% reflects efficient biomass conversion into biochar, demonstrating effective utilization of the material during the pyrolysis process. The high elemental carbon content (89.66%) confirms the production of highly carbonized biochar, while the calculated fixed carbon content (84.97%), derived as 100% minus volatile matter (6.83%) and ash (8.20%), represents the fraction of carbon expected to remain stable in soil over long periods. The difference between elemental carbon (89.66%) and fixed carbon (84.97%) is attributed to residual carbon-containing volatile compounds that are released upon further heating. This fixed carbon value (84.97%) is the primary parameter for assessing carbon sequestration potential, as it corresponds to the recalcitrant, non-labile carbon fraction resistant to microbial decomposition [14].

Low hydrogen (1.31%), nitrogen (0.132%), and oxygen (6.86%) contents suggest that the biochar has a predominantly aromatic structure with reduced chemical reactivity, enabling its prolonged presence in soil without rapid degradation [80]. Reduced volatile matter content (6.83%) indicates thermal stability, while low sulfur content (0.031%) minimizes environmental risks such as soil acidification. The high calorific value (7504.79 kcal/kg) underscores its potential as a solid biofuel for energy applications. The presence of ash (8.20%) and silica (2.83%) could positively influence soil fertility by aiding nutrient retention and improving soil structure, but this hypothesis requires direct testing through soil incubation or plant growth experiments.

The X-ray diffraction analysis (Figure 11) of *Dendrocalamus strictus* biochar revealed a crystallinity index of 30.16%, indicating the presence of both crystalline and amorphous regions in its structure [79]. This value suggests that, while the biochar contains an ordered fraction, a significant portion of its structure remains disorganized, a characteristic typical of carbonized materials derived from lignocellulosic biomass [80,81]. The amorphous fraction is usually associated with disordered carbon, which can directly influence its adsorption properties and interaction with soil.

Based on literature reports, the presence of a partially crystalline structure is expected to enhance the stability of biochar in soil, potentially reducing its decomposition over time and enabling more long-lasting carbon sequestration. Additionally, the amorphous fraction has been associated with improved nutrient and contaminant adsorption, which could position biochar as both a soil conditioner and a potential agent for environmental

remediation. However, these effects remain to be verified for the specific biochar produced in this study through targeted agronomic assays [82]. Additionally, the amorphous fraction tends to improve nutrient and contaminant adsorption, positioning biochar as both a soil conditioner and a potential agent for environmental remediation [83]. These combined characteristics suggest that *Dendrocalamus strictus* biochar can play a dual role in soil: improving its physicochemical properties while acting as a stable carbon reservoir, contributing to climate change mitigation [84].

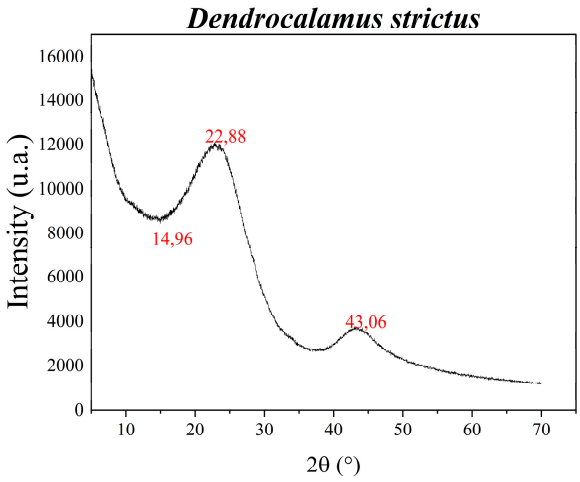

Figure 11. X-ray diffractograms of *Dendrocalamus strictus* biochar.

The mass loss as a function of increasing temperature for the produced biochar can be observed in Figure 12.

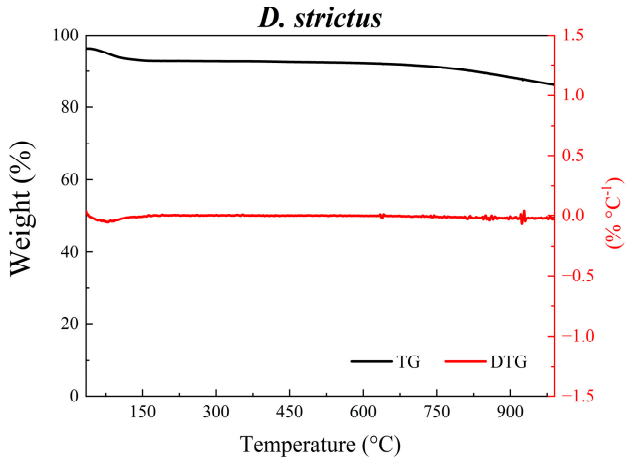

Figure 12. TG/DTG curves of *Dendrocalamus strictus* biochars.

The thermogravimetric curve (TG) and derivative thermogravimetric curve (DTG) of *Dendrocalamus strictus* biochar, presented in Figure 12, illustrate its thermal stability and behavior under increasing temperatures. The biochar demonstrates relatively low mass loss throughout the analyzed temperature range, indicating high thermal resistance. This trait is attributed to its high fixed carbon content and prior degradation of volatile matter during pyrolysis, making the biochar more resistant to thermal decomposition [85,86].

The DTG curve (in red) shows no significant peaks of mass loss, further confirming the thermal stability of the biochar. This advantageous behavior enhances its suitability for soil applications, as it suggests slow degradation and the ability to act as a stable carbon reservoir over extended periods. Additionally, its low decomposition rate can improve soil

physicochemical properties without frequent replenishments, positioning *Dendrocalamus strictus* biochar as a sustainable option for agricultural management and carbon emission mitigation [87,88]. Considering the application of biochar in soil, analyses of surface area and pore structure were conducted, and the results are presented in Table 17.

Table 17. Surface area and pore characteristics of the biochar.

Species	BET Surface Area (m^2/g)	Total Pore Volume (cm^3/g)	Average Pore Diameter (nm)
D. strictus	120.154	0.085	2.822

The BET surface area analysis, total pore volume, and average pore diameter of *Dendrocalamus strictus* biochar reveal favorable properties for soil application. Its high specific surface area (120.154 m^2/g) indicates a highly porous material, which according to the literature could contribute to water and nutrient retention in the soil, potentially reducing leaching and improving the availability of essential elements for plants. Nevertheless, direct evidence for these agronomic benefits is not provided in the present study, and such effects would need to be confirmed through controlled soil or plant assays. This feature may be beneficial in sandy or degraded soils, but this remains a hypothesis to be tested [87]. This feature is particularly beneficial in sandy or degraded soils, where low water retention capacity hinders crop growth.

Additionally, the total pore volume (0.085 cm^3/g) and average pore diameter (2.822 nm) indicate a predominantly mesoporous structure, which promotes the colonization of beneficial microorganisms and the adsorption of organic and inorganic compounds. The presence of mesopores facilitates gas exchange within the soil and enhances biological activity, improving the health of the underground ecosystem. Thus, *Dendrocalamus strictus* biochar exhibits characteristics that not only enhance soil physicochemical properties but also contribute to mitigating environmental impacts, making it a promising alternative for sustainable agriculture [89–91].

3.7. Technical–Economic Assessment (TEA)

According to the literature, on an industrial scale, the pyrolysis of bamboo yields a biochar range of 30–35% [12–14]. Based on the experimental gravimetric yield of 31.14% for *Dendrocalamus strictus*, a preliminary techno-economic assessment was conducted. Table 18 summarizes the key parameters and the estimated profit per ton and per hectare. The calculation assumes a 3-year rotation cycle, a unified biochar selling price of US$ 120/ton, and a production cost of US$ 31.14/ton of biochar. All values are presented as point estimates. This is a preliminary estimate intended to provide a first indication of economic feasibility; it does not include sensitivity analysis, discount rates, or net present value calculations. Future work should include a full techno-economic model with uncertainty and sensitivity analysis [41].

The techno-economic analysis of Dendrocalamus strictus biochar reveals a significant profit per ton (US 88.86) and per hectare (US 1107), indicating strong economic viability for this biomass production. A 31.14% biochar yield, combined with a revenue of US 48.3 per ton and relatively low costs (US31.14), contributes to considerable profitability. Additionally, the basic density of 0.517 t/m^3 suggests efficient production with good material utilization. These results are promising, especially when considering the 3-year rotation cycle, which enables continuous and profitable production. However, it is important to note that the market viability of biochar (price of US$120/ton) and other operational costs may influence profits, depending on price fluctuations and expenses associated with production and commercialization [92].

Table 18. Technical–Economic Assessment of *Dendrocalamus strictus* biochar in terms of Profit (US$/t and US$/ha).

Parameter	Value	Unit	Source
Basic density	0.517	t/m^3	Experimental (Table 9)
Biomass productivity	40	ton/ha/year	Estimated from density and rotation
Biochar gravimetric yield	31.14	%	Experimental (Table 16)
Biochar production	12.456	ton/ha/year	=Biomass × Yield (%)
Biochar selling price	120.00	US$/ton	Market price (agricultural grade, Brazil 2024)
Operational cost	31.14	US$/ton	Based on [37,38]
Revenue per ton	120.00	US$/ton	=Selling price
Cost per ton	31.14	US$/ton	=Operational cost
Profit per ton	88.86	US$/ton	=Revenue − Cost
Profit per hectare per year	1107	US$/ha/year	=Profit per ton × Biochar production

3-year rotation cycle. All values are point estimates. This is a preliminary assessment; sensitivity analysis, discount rates, and NPV are not included.

3.8. Biochar Application

Based on the characterization of biochar produced from *Dendrocalamus strictus*, its application in soil offers numerous agronomic and environmental benefits. The high fixed carbon content (84.97%) and porous structure of the biochar enhance water and nutrient retention in the soil, reducing losses from leaching and increasing fertilizer use efficiency [93]. Furthermore, its low reactivity and chemical stability ensure prolonged effects in the soil, contributing to long-term improvements in fertility. These factors make the biochar from *Dendrocalamus strictus* an excellent choice for degraded soils or those with low moisture retention capacity [94].

In addition to its physicochemical benefits, the application of biochar from this species also aids in mitigating climate change, as the carbon sequestered in bamboo biomass is stabilized in the soil for extended periods, reducing CO_2 emissions into the atmosphere [95]. Studies have shown that biochar can stimulate plant growth by creating an environment more conducive to beneficial microbial activity, improving soil health and enhancing agricultural productivity [96]. Consequently, the use of *Dendrocalamus strictus* biochar stands out as a sustainable alternative for regenerative agriculture and soil management.

4. Conclusions

The study revealed significant radial variability in anatomical, chemical, and physical properties across the four bamboo species (*Dendrocalamus strictus*, *Dendrocalamus asper*, *Guadua chacoensis*, and *Bambusa nutans*). *Dendrocalamus strictus* exhibited higher proportions of parenchyma and lignin, particularly in the peripheral region, while other species showed greater fiber content. Basic density and fiber morphology varied radially, with the highest densities observed in the periphery.

Dendrocalamus strictus emerged as the most promising species for biochar production due to its high lignin content (30.40%), thermal stability, and favorable gravimetric yield (31.14%). The biochar demonstrated excellent physicochemical properties, including high elemental carbon (89.66%) and a calculated fixed carbon content of 84.97% (derived from proximate analysis), low volatiles (6.83%), and a mesoporous structure (120 m^2/g surface area), suggesting its potential suitability for soil conditioning and carbon sequestration. Direct agronomic validation is required to confirm these hypothesized benefits.

A preliminary techno-economic assessment (TEA) indicated a potential profit of approximately US$ 89/ton and US$ 1107/hectare per year for *Dendrocalamus strictus* biochar under a 3-year rotation cycle, assuming a biochar price of US$ 120/ton. However, this estimate is preliminary and does not include sensitivity analysis. Future studies should

perform a full TEA with uncertainty quantification (e.g., variation in biochar price, yield, and transportation costs) to confirm commercial viability under different market scenarios. These findings highlight the dual potential of bamboo as a sustainable resource for agro-industrial applications, combining ecological benefits with economic feasibility. Future research should explore biochar interactions with different soils and crops to optimize its agricultural use. However, because *Dendrocalamus asper* originated from a different geographic location than the other three species, the comparative findings should be considered preliminary regarding species-level differences. Future studies should standardize collection sites or include controlled cultivation experiments to confirm the observed patterns.

5. Future Work

For future studies, it is recommended to conduct additional research on the interaction of *Dendrocalamus strictus* biochar with various soil types and agricultural crops to optimize its application and maximize agronomic benefits. Additionally, producing and characterizing biochar derived from other bamboo species could provide valuable insights. Further investigations into the effects of this biochar on soil microbial communities and nutrient dynamics are also suggested, offering a deeper understanding of its long-term impacts [97]. Exploring its potential for remediating contaminated soils and integrating biochar usage with other sustainable practices, such as composting and organic fertilization, represents another promising research avenue. Lastly, analyzing the economic and environmental feasibility of large-scale biochar implementation could contribute to the development of public policies and strategies, promoting its use in agriculture and sustainable soil management [98]. Additionally, a comprehensive techno-economic assessment including sensitivity analysis (e.g., ±20% variation in biochar price, ±5% in gravimetric yield, and transportation costs) and life-cycle costing (discount rates, net present value) is recommended to support commercial-scale decisions regarding *Dendrocalamus strictus* biochar.

Supplementary Materials: The following supporting information can be downloaded at: https://www.mdpi.com/article/10.3390/bioresourbioprod2020010/s1, Table S1. Information on Bamboo Species; Figure S1. Anatomical Variations Along the Culm Wall (Source: Author's Own Work). Figure S2. Culm of Dendrocalamus strictus Highlighting the Distribution of Vascular Bundles (Source: Author's Own Work). Figure S3. Frequency of Vascular Elements in *Dendrocalamus strictus* by Radial Position (A-Periphery, B-Center, C-Inner Culm Wall) (Source: Author's Own Work). Figure S4. Frequency of Vascular Elements in *Dendrocalamus aspers* by Radial Position (A-Periphery, B-Center, C-Inner Culm Wall) (Source: Author's Own Work). Figure S5. Frequency of Vascular Elements in *Guadua chacoensis* by Radial Position (A-Periphery, B-Center, C-Inner Culm Wall) (Source: Author's Own Work). Figure S6. Frequency of Vascular Elements in *Bambusa nutans* by Radial Position (A-Periphery, B-Center, C-Inner Culm Wall) (Source: Author's Own Work). Table S2. Average Fiber Proportion Values Based on Radial Position. Table S3. Average Fiber Values by Species. Table S4. Average Values of Carbon, Hydrogen, and Oxygen in Bamboo Biomass Based on Culm Position. Table S5. Nitrogen and Sulfur Content (%) in Bamboo Species.

Author Contributions: K.S.A., writing—review & editing, writing—original draft, visualization, validation, supervision, software, resources, project administration, methodology, investigation, funding acquisition, formal analysis, data curation, conceptualization; T.G., writing—review & editing, writing—original draft, visualization, validation, supervision, software, resources, project administration, methodology, investigation, funding acquisition, formal analysis, data curation, conceptualization; A.d.C.O.C., writing—review & editing, writing—original draft, visualization, validation, supervision, project administration, funding acquisition; A.M.M.L.C., writing—review & editing, writing—original draft, visualization, validation, supervision, project administration, funding acquisition; S.R.V., writing—review & editing, writing—original draft, visualization, valida-

tion, supervision, project administration, funding acquisition; M.M.d.C., writing—review & editing, writing—original draft, visualization, validation, supervision, project administration, funding acquisition. All authors have read and agreed to the published version of the manuscript.

Funding: This research was funded by FAPEMIG, CNPq/FAPEMIG agreement recorded in SICONV: 793988/2013 and INCT Midas and CAPES—Finance Code 001. SAF is supported by research fellowships from CNPq.

Institutional Review Board Statement: Not applicable.

Informed Consent Statement: Not applicable.

Data Availability Statement: The original contributions presented in this study are included in the article/Supplementary Materials. Further inquiries can be directed to the corresponding author(s).

Conflicts of Interest: The authors declare no conflicts of interest.

References

1. Patel, H.R.; Mathakia, R.; Mangroliya, U.C.; Mandaliya, V.B. Sustainable bamboo: Technological innovations and patent insights for a greener future. *Adv. Bamboo Sci.* **2025**, *10*, 100127. [CrossRef]
2. Isukuru, E.J.; Ogunkeyede, A.O.; Adebayo, A.A.; Uruejoma, M.F. Potentials of bamboo and its ecological benefits in Nigeria. *Adv. Bamboo Sci.* **2023**, *4*, 100032. [CrossRef]
3. Ahmad, Z.; Upadhyay, A.; Ding, Y.; Emamverdian, A.; Shahzad, A. Bamboo: Origin, Habitat, Distributions and Global Prospective. In *Biotechnological Advances in Bamboo: The "Green Gold" on the Earth*; Springer Nature: Berlin/Heidelberg, Germany, 2021; pp. 1–31.
4. Boadu, K.B.; Ansong, M.; Afrifah, K.A.; Nsiah-Asante, E. Pulp and Paper Making Characteristics of Fibers from Plantation-grown Oxythenantera Abyssinica and Beema Bamboo (A Tissue Cultured Clone from Bambusa Balcooa). *J. Nat. Fibers* **2022**, *19*, 4198–4209. [CrossRef]
5. Kumar, S.; Rawat, D.; Singh, B.; Khanduri, V.P. Utilization of bamboo resources and their market value in the western Himalayan region of India. *Adv. Bamboo Sci.* **2023**, *3*, 100019. [CrossRef]
6. Piazza, M.; Lobovikov, M. *World Bamboo Resources—A Thematic Study Prepared in the Framework of the Global Forest Resources Assessment 2005*; Food and Agriculture Organization (FAO): Rome, Italy, 2007. [CrossRef]
7. Maitra, S.; Singh, V. Invited review on 'maize in the 21st century' Emerging trends of maize biorefineries in the 21st century: Scientific and technological advancements in biofuel and bio-sustainable market. *J. Cereal Sci.* **2021**, *101*, 103272. [CrossRef]
8. Akinlabi, E.T.; Anane-Fenin, K.; Akwada, D.R. Regeneration, Cultivation, and Sustenance of Bamboo. In *Bamboo*; Springer International Publishing: Berlin/Heidelberg, Germany, 2017; pp. 39–86.
9. Emi Rainildes Lorenzetti, T.K.C.; de André Bacic Olic, P.C.O.; Rodrigo de Oliveira Almeida, R.C.M. Bamboo as a resource to social technology at zona da mata of Minas Gerais. In *Bambus No Brasil: Da Biologia à Tecnologia*; Instituto Ciência Hoje (ICH): Rio de Janeiro, Brazil, 2017; pp. 307–320.
10. Santi, T. O potencial do bambu: Desafios e oportunidades da fibra na produção de celulose e papel e as novas pesquisas sobre seu uso para fins energéticos e geração de biomateriais. *Rev. Tecnol. Celul. Pap.* **2015**, *4*, lxxvi.
11. Long, L.; Yu, M.; Yao, W.; Ding, Y.; Lin, S. Research advance in growth and development of bamboo organs. *Ind. Crops Prod.* **2023**, *205*, 117428. [CrossRef]
12. Lin, L.-D.; Chang, F.-C.; Ko, C.-H.; Wang, C.-T. Bamboo-Derived Fuel from Dendrocalamus latiflorus, Phyllostachys makinoi, and Phyllostachys pubescens Waste. *BioResources* **2016**, *11*, 8425–8434. [CrossRef]
13. Viglašová, E.; Galamboš, M.; Danková, Z.; Krivosudský, L.; Lengauer, C.L.; Hood-Nowotny, R.; Soja, G.; Rompel, A.; Matík, M.; Briančin, J. Production, characterization and adsorption studies of bamboo-based biochar/montmorillonite composite for nitrate removal. *Waste Manag.* **2018**, *79*, 385–394. [CrossRef]
14. Alves, K.S.; Guimarães, T.; de Carvalho Bittencout, R.; Gonçalves, P.A.R.; de Cássia Oliveira Carneiro, A.; Carvalho, A.M.M.L.; da Costa, M.M. Bamboo-derived biochars: Physicochemical properties and implications for soil fertility and sustainability. *Biomass Convers. Biorefinery* **2025**, *15*, 21085–21105. [CrossRef]
15. Marafon, A.C.; Amaral, A.F.C.; De Lemos, E.E.P. Characterization of bamboo species and other biomasses with potential for thermal energy generation. *Pesqui. Agropecu. Trop.* **2019**, *49*, e55282. [CrossRef]
16. Liang, Z.; Neményi, A.; Kovács, G.P.; Gyuricza, C. Potential use of bamboo resources in energy value-added conversion technology and energy systems. *GCB Bioenergy* **2023**, *15*, 936–953. [CrossRef]
17. Aziz, S.A.; Sarjadi, M.S. A Brief Overview of the Use of Bamboo Biomass in the Asian Region's Energy Production. *Cellulose* **2023**, *2023*, 7–26.

18. Daza Montaño, C. *Potential of Bamboo for Renewable Energy: Main Issues and Technology Options*; International Bamboo and Rattan Organisation (INBAR): Beijing, China, 2021.
19. do Nascimento, Í.V.; Fregolente, L.G.; de Pereira, A.P.A.; do Nascimento, C.D.V.; Mota, J.C.A.; Ferreira, O.P.; de Freitas Sousa, H.H.; da Silva, D.G.G.; Simões, L.R.; Souza Filho, A.G.; et al. Biochar as a carbonaceous material to enhance soil quality in drylands ecosystems: A review. *Environ. Res.* **2023**, *233*, 116489. [CrossRef]
20. Hernandez-Mena, L.E.; Pecora, A.A.B.; Beraldo, A.L. Slow pyrolysis of bamboo biomass: Analysis of biochar properties. *Chem. Eng. Trans.* **2014**, *37*, 115–120. [CrossRef]
21. Rusch, F.; de Abreu Neto, R.; de Moraes Lúcio, D.; Hillig, É. Energy properties of bamboo biomass and mate co-products. *SN Appl. Sci.* **2021**, *3*, 602. [CrossRef]
22. do Vale, A.T.; de Oliveira Moreira, A.C.; Martins, I.S. Evaluation of *Bambusa vulgaris* Energy Potential Based on Age. *Floresta Ambiente* **2017**, *24*, e00123314. [CrossRef]
23. Al-Rumaihi, A.; Shahbaz, M.; Mckay, G.; Mackey, H.; Al-Ansari, T. A review of pyrolysis technologies and feedstock: A blending approach for plastic and biomass towards optimum biochar yield. *Renew. Sustain. Energy Rev.* **2022**, *167*, 112715. [CrossRef]
24. Luan, Y.; Ma, Y.F.; Liu, L.T.; Fei, B.H.; Fang, C.H. A novel bamboo engineering material with uniform density, high strength, and high utilization rate. *Ind. Crops Prod.* **2022**, *184*, 115045. [CrossRef]
25. Maia Aveiro Cessa, R.; Celi, L.; Carlos Tadeu Vitorino, A.; Novelino, J.O.; Barberis, E. Área superficial específica, porosidade da fração argila e adsorção de fósforo em dois latossolos vermelhos. *Rev. Bras. Ciênc. Solo* **2009**, *33*, 1153–1162. [CrossRef]
26. Baba, S.; Imasato, K.; Yamamoto, A.; Ishida, T.; Ohta, M. Integrating thermoelectric devices in pyrolysis reactors for biochar and electricity co-production. *Energy Convers. Manag. X* **2024**, *24*, 100725. [CrossRef]
27. Brand, M.A.; Rodrigues, A.A.; de Oliveira, A.; Machado, M.S.; Zen, L.R. Qualidade do carvão vegetal para o consumo doméstico comercializado na região serrana sul de santa catarina. *Rev. Arvore* **2015**, *39*, 1165–1173. [CrossRef]
28. Liese, W.; Tang, T.K.H. *Properties of the Bamboo Culm*; Springer: Berlin/Heidelberg, Germany, 2015.
29. Rusch, F.; Hillig, É.; Trevisan, R.; Mustefaga, E.C.; Campos, R.F. Propriedades físicas e mecânicas de hastes adultas de diferentes espécies de bambu: Uma revisão. *Braz. J. Dev.* **2020**, *6*, 22549–22566. [CrossRef]
30. Camargo Caicedo, Y.; Arango, J.A.M.; Muriel, A.P. Anato-morphological and chemical characterization of bamboo (*Guadua amplexifolia* J. Presl) from San Jorge River Basin, Colombia. *Clean. Eng. Technol.* **2025**, *24*, 100884. [CrossRef]
31. Andrade Bueno, I.G.; de Picoli, E.A.T.; dos Isaias, R.M.S.; Lopes-Mattos, K.L.B.; Cruz, C.D.; Kuki, K.N.; Zauza, E.A.V. Wood anatomy of field grown eucalypt genotypes exhibiting differential dieback and water deficit tolerance. *Curr. Plant Biol.* **2020**, *22*, 100136. [CrossRef]
32. *TAPPI T264 om-88*; Preparation of Wood for Chemical Analysis. TAPPI Press: Atlanta, GA, USA, 1998.
33. *TAPPI T204 om-88*; Solvent Extractives of Wood and Pulp. TAPPI Press: Atlanta, GA, USA, 2001.
34. *TAPPI T222 om-97*; Acid-Insoluble Lignin in Wood and Pulp. TAPPI Press: Atlanta, GA, USA, 1997.
35. *TAPPI T211 om-97*; Ash in Wood, Pulp, Paper and Paperboard: Combustion at 525 °C. TAPPI Press: Atlanta, GA, USA, 1998.
36. *TAPPI T266 om-94*; Determination of Sodium, Calcium, Copper, Iron and Manganese in Wood and Pulp by Atomic Absorption Spectroscopy. TAPPI Press: Atlanta, GA, USA, 1998.
37. Barbosal, L.; Maltha, C.; Silva, V.; Colodette, J. Determinação Da relação siringila/guaiacila Da lignina em maDeiras De eucalipto por pirólise acoplaDa à cromatografia gasosa e espectrometria De massas (pi-cg/em). *Artig. Quím. Nova* **2008**, *31*, 2035–2041. [CrossRef]
38. da Silva, S.H.F.; Gordobil, O.; Labidi, J. Organic acids as a greener alternative for the precipitation of hardwood kraft lignins from the industrial black liquor. *Int. J. Biol. Macromol.* **2020**, *142*, 583–591. [CrossRef] [PubMed]
39. Sahoo, S.S.; Vijay, V.K.; Chandra, R.; Kumar, H. Production and characterization of biochar produced from slow pyrolysis of pigeon pea stalk and bamboo. *Clean. Eng. Technol.* **2021**, *3*, 100101. [CrossRef]
40. de Bittencourt, R.C.; Guimarães, T.; da Costa, M.M.; Silva, L.S.; Barbosa, V.O.d.P.; Arêdes, S.C.d.L.; Alves, K.S.; Carvalho, A.M.M.L. Production of High-Value Green Chemicals via Catalytic Fast Pyrolysis of Eucalyptus urograndis Forest Residues. *Sustainability* **2024**, *16*, 8294. [CrossRef]
41. Guimarães, T.; Bittencourt, R.C.; Carvalho, A.M.M.L.; Valverde, S.R.; da Costa, M.M. Technical-economic assessment of 5-hydroxymethylfurfural production via catalytic hydrothermal synthesis from lignocellulosic forest residues. *Food Bioprod. Process.* **2024**, *148*, 341–352. [CrossRef]
42. Ghavami, K.; Perazzo Barbosa, N.; Eustáquio Moreira, L. Bambu como Material de Engenharia. In *Avaliação de Desempenho de Tecnologias Construtivas Inovadoras: Conforto Ambiental, Durabilidade e Pós-Ocupação*; Editora Scienza: São Paulo, Brazil, 2017; pp. 305–348.
43. Sola, G.S.; da Costa, M.R.N.; de Alcantara, B.K. Descrição morfológica e caracterização anatômica do colmo maduro do bambu gigante da Amazônia (Guadua aff. lynnclarkiae). *Ed. Licuri* **2023**, *2023*, 180–194.
44. Karlinasari, L. Pengaruh Komponen Kimia Dan Ikatan Pembuluh Terhadap Kekuatan Tarik Bambu. 2016, Volume 23, No. 1. ISSN 0853-2982. Available online: https://d1wqtxts1xzle7.cloudfront.net/45267047/4.-Effendi-Tri-Bahtiar-dkk-Vol.23-No.1-Hal-31-40-

libre.pdf?1462173790=&response-content-disposition=inline%3B+filename%3DPengaruh_Komponen_Kimia_dan_Ikatan_Pembu.pdf&Expires=1780550183&Signature=RIZBb7DuyFiiAjfDfAZc9uIRyYlx6k3kaBLQWEY8FBUZVgbSAJH6LNGBfkcOWA93ZuttqhbIRIGoilbfuhguvn3b84ljKnPkoZiOt5PwGA1mQSIMpCJMOMZNbqxEBG11 fgwX1lgf51 XmgJWFBXUcEL11awSpCyLlwysjcHcmYnQ0oajR86D7wzprDvgeN5tXlkPOkkyPpNRRwIYSM79yXR cTAIa23oool62fV9F5WPFlNFAu4HQzfL0DyemwO5haxcNrnPI4cNUXQRRPL5qSDp1eOvLvtnfsFSr0kpn-0I 84 uF5GVHXkA5i0yUpmhFBJUIsAW02-K7nQORjbw__&Key-Pair-Id=APKAJLOHF5GGSLRBV4ZA (accessed on 30 May 2026).
45. Agustí, J.; Blázquez, M.A. Plant vascular development: Mechanisms and environmental regulation. *Cell. Mol. Life Sci.* **2020**, *77*, 3711–3728. [CrossRef]
46. Timell, T.E.; Berlin, S.-V.; Gmbh, H. *Springer Series in Wood Science*; Springer Nature: Berlin/Heidelberg, Germany, 1983.
47. Grosser, D.; Liese, W. *On the Anatomy of Asian Bamboos, with Special Reference to Their Vascular Bundles*; Springer: Berlin/Heidelberg, Germany, 1971.
48. Huang, X.; Li, F.; De Hoop, C.F.; Jiang, Y.; Xie, J.; Qi, J. Analysis of bambusa rigida bamboo culms between internodes and nodes: Anatomical characteristics and physical-mechanical properties. *Prod. J.* **2018**, *68*, 157–162. [CrossRef]
49. Brito, F.M.S.; Paes, J.B.; da Oliveira, J.T.S.; Arantes, M.D.C.; Neto, H.F. Caracterização anatômica e física do bambu gigante (*Dendrocalamus giganteus* Munro). *Floresta Ambiente* **2015**, *22*, 559–566. [CrossRef]
50. Filho, M.T. *Estrutura Anatômica, Dimensões das Fibras e Densidade Básica de Colmos de Bambusa Vulgaris Schrad*; Instituto de Pesquisas e Estudos Florestais: São Paulo, Brasil, 1987.
51. Liese, W. Liese Walter. In *The Anatomy of Bamboo Culms*; Brill Academic Publishers: Berlin, Germany, 2002.
52. 500559747-1992-CORADIN-MUNIZ-Normas-e-Procedimentos-Em-Estudos-de-Anatomia-Da-Madeira. Available online: https://www.scribd.com/document/500559747/1992-CORADIN-MUNIZ-Normas-e-Procedimentos-Em-Estudos-de-Anatomia-Da-Madeira (accessed on 30 May 2026).
53. França, T.S.F.A.; Arantes, M.D.C.; Paes, J.B.; Vidaurre, G.B.; Oliveira, J.T.d.S.; Baraúna, E.E.P. Características anatômicas e propriedades físico-mecânicas das madeiras de duas espécies de mogno Africano. *Cerne* **2015**, *21*, 633–640. [CrossRef]
54. Ciaramello, D.; Azzini, A. Bambu Como Matéria-prima para papel: III-es-Tudos Sôbre o Emprego de Quatro Espécies de Bambus a, na Produção de Celulose Sul-Fato (1). *Bragantia* **1971**, *30*, 199–213. [CrossRef]
55. Siam, N.A.; Uyup, M.K.A.; Husain, H.; Mohmod, A.L.; Awalludin, M.F. Anatomical, physical, and mechanical properties of thirteen Malaysian bamboo species. *Bioresources* **2019**, *14*, 3925–3943. [CrossRef]
56. Santos, D.R.S.; Sette, C.R.; Da Silva, M.F.; Yamaji, F.M.; Almeida, R.d.A. Potencial de espécies de Bambu como fonte energética. *Sci. For.* **2016**, *44*, 751–758. [CrossRef]
57. Árvore, R.; Viçosa, M. Potencial energetico da madeira de eucalyptus sp. em. . . Potencial energético da madeira de Eucalyptus sp. em função da idade e de diferentes materiais genéticos. Potential energy of *Eucalyptus* sp. wood according to age and different genetic materials. *Rev. Árvore* **2014**, *38*, 375–381.
58. Wilson, L.; Yang, W.; Blasiak, W.; John, G.R.; Mhilu, C.F. Thermal characterization of tropical biomass feedstocks. In *Energy Conversion and Management*; Elsevier Ltd.: Amsterdam, The Netherlands, 2011; pp. 191–198.
59. Genovese, A.L. Aspectos Energéticos da Biomassa Como Recurso No Brasil e No Mundo. In *Proceedings of the 6. Encontro de Energia no Meio Rural*; SciELO Proceedings: São Paulo, Brazil, 2006.
60. de Carvalho, S.R. Danilo Campiom Arantes Bagaço de Cana-de-Açúcar: Análise Térmica e Energética de Biomassa Mestre em Engenharia Mecânica. Área de Concentração: Transferência de Calor e Mecânica dos Fluidos. 2014. Available online: https://repositorio.ufu.br/handle/123456789/14971 (accessed on 30 May 2026).
61. Potenciano Marinho, N.; Nisgoski, S.; Klock, U.; Andrade, A.S.D.; Muñiz, G.I.B.D. Análise química do bambu-gigante (*Dendrocalamus giganteus* wall. ex munro) em diferentes idades. *Ciência Florest.* **2012**, *22*, 417–422. [CrossRef]
62. Rusch, F.; Dirceu Wastowski, A.; Shimosakai de Lira, T.; Moreira, K.C.C.S.R.; de Moraes Lúcio, D. Description of the component properties of species of bamboo: A review. *Biomass-Convers. Biorefinery* **2021**, *13*, 2487–2495. [CrossRef]
63. Zhang, Z.; Rao, F.; Wang, Y. Morphological, Chemical, and Physical–Mechanical Properties of a Clumping Bamboo (*Thyrsostachys oliveri*) for Construction Applications. *Polymers* **2022**, *14*, 3681. [CrossRef]
64. Wahab, R.; Mustafa, M.T.; Sudin, M.; Mohamed, A.; Rahman, S.; Samsi, H.W.; Khalid, I. Extractives, Holocellulose, a-Cellulose, Lignin and Ash Contents in Cultivated Tropical Bamboo *Gigantochloa brang*, *G. levis*, *G. scortechinii* and *G. wrayi*. *Curr. Res. J. Biol. Sci.* **2013**, *5*, 266–272. [CrossRef]
65. Santos, A.R.C.D.S. Caracterização Tecnológica de Espécies de Bambu Visando a Produção de Polpa Celulósica. Tese de Doutorado, Universidade de São Paulo, São Paulo, Brazil, 2023.
66. Yang, H.; Yan, R.; Chen, H.; Lee, D.H.; Zheng, C. Characteristics of hemicellulose, cellulose and lignin pyrolysis. *Fuel* **2007**, *86*, 1781–1788. [CrossRef]
67. Boerjan, W.; Ralph, J.; Baucher, M. Lignin Biosynthesis. *Annu. Rev. Plant Biol.* **2003**, *54*, 519–546. [CrossRef]
68. de Ferreira, S.O.P.M.; Ferreira Júnior, J.A.M.; Braz, R.L. Energy characterization of agricultural and forestry biomasses in the state of Pernambuco. *Cienc. Florest.* **2024**, *34*, e73324. [CrossRef]

69. Sannigrahi, P.; Ragauskas, A.J.; Tuskan, G.A. Poplar as a feedstock for biofuels: A review of compositional characteristics. *Biofuels Bioprod. Biorefining* **2010**, *4*, 209–226. [CrossRef]
70. Pu, Y.; Hu, F.; Huang, F.; Davison, B.H.; Ragauskas, A.J. Assessing the molecular structure basis for biomass recalcitrance during dilute acid and hydrothermal pretreatments. *Biotechnol. Biofuels* **2013**, *6*, 15. [CrossRef] [PubMed]
71. Abdi, H.; Williams, L.J. Principal Component Analysis. *Technometrics* **2003**, *45*, 276. [CrossRef]
72. Priyadarshi, R.; Ghosh, T.; Purohit, S.D.; Prasannavenkadesan, V.; Rhim, J.-W. Lignin as a sustainable and functional material for active food packaging applications: A review. *J. Clean. Prod.* **2024**, *469*, 143151. [CrossRef]
73. Ali, S.; Rani, A.; Dar, M.; Qaisrani, M.M.; Noman, M.; Yoganathan, K.; Asad, M.; Berhanu, A.; Barwant, M.; Zhu, D. Recent Advances in Characterization and Valorization of Lignin and Its Value-Added Products: Challenges and Future Perspectives. *Biomass* **2024**, *4*, 947–977. [CrossRef]
74. Zevallos Torres, L.A.; Lorenci Woiciechowski, A.; de Andrade Tanobe, V.O.; Karp, S.G.; Lorenci, L.C.G.; Faulds, C.; Soccol, C.R. Lignin as a potential source of high-added value compounds: A review. *J. Clean. Prod.* **2020**, *263*, 121499. [CrossRef]
75. Wu, Y.; Gui, Q.; Zhang, H.; Li, H.; Li, B.; Liu, M.; Chen, Y.; Zhang, S.; Yang, H.; Chen, H. Effect of biomass components' interaction on the pyrolysis reaction kinetics and small-molecule product release characteristics. *J. Anal. Appl. Pyrolysis* **2023**, *173*, 106039. [CrossRef]
76. Zhang, Y.; Liang, Y.; Li, S.; Yuan, Y.; Zhang, D.; Wu, Y.; Xie, H.; Brindhadevi, K.; Pugazhendhi, A.; Xia, C. A review of biomass pyrolysis gas: Forming mechanisms, influencing parameters, and product application upgrades. *Fuel* **2023**, *347*, 128461. [CrossRef]
77. Hu, X.; Gholizadeh, M. Biomass pyrolysis: A review of the process development and challenges from initial researches up to the commercialisation stage. *J. Energy Chem.* **2019**, *39*, 109–143. [CrossRef]
78. Berbenni, V.; Marini, A. Thermogravimetry and X-ray diffraction study of the thermal decomposition processes in Li_2CO_3-$MnCO_3$ mixtures. *J. Anal. Appl. Pyrolysis* **2002**, *62*, 45–62. [CrossRef]
79. Al Garawi, M.S.; Al Salman, S.A.; Mansoor, A.S.; Kayani, A.; Al-Ghamdi, S.; Baig, M. X-ray diffraction (XRD), thermogravimetric analysis (TGA) and impedance spectroscopy studies of PM-355 as a function of proton fluence. *Radiat. Meas.* **2017**, *99*, 41–43. [CrossRef]
80. Liang, J.F.; Li, Q.W.; Gao, J.Q.; Feng, J.G.; Zhang, X.Y.; Hao, Y.J.; Yu, F.H. Biochar-compost addition benefits Phragmites australis growth and soil property in coastal wetlands. *Sci. Total Environ.* **2021**, *769*, 145166. [CrossRef]
81. Bunaciu, A.A.; Udriştioiu, E.; Aboul-Enein, H.Y. X-Ray Diffraction: Instrumentation and Applications. *Crit. Rev. Anal. Chem.* **2015**, *45*, 289–299. [CrossRef]
82. Yao, W.; Weng, Y.; Catchmark, J.M. Improved cellulose X-ray diffraction analysis using Fourier series modeling. *Cellulose* **2020**, *27*, 5563–5579. [CrossRef]
83. Ju, X.; Bowden, M.; Brown, E.E.; Zhang, X. An improved X-ray diffraction method for cellulose crystallinity measurement. *Carbohydr. Polym.* **2015**, *123*, 476–481. [CrossRef]
84. Allohverdi, T.; Mohanty, A.K.; Roy, P.; Misra, M. A review on current status of biochar uses in agriculture. *Molecules* **2021**, *26*, 5584. [CrossRef]
85. Singh Yadav, S.P.; Bhandari, S.; Bhatta, D.; Poudel, A.; Bhattarai, S.; Yadav, P.; Ghimire, N.; Paudel, P.; Shrestha, J.; Oli, B. Biochar application: A sustainable approach to improve soil health. *J. Agric. Food Res.* **2023**, *11*, 100498. [CrossRef]
86. Bolan, S.; Hou, D.; Wang, L.; Hale, L.; Egamberdieva, D.; Tammeorg, P.; Li, R.; Wang, B.; Xu, J.; Wang, T.; et al. The potential of biochar as a microbial carrier for agricultural and environmental applications. *Sci. Total Environ.* **2023**, *886*, 163968. [CrossRef] [PubMed]
87. Afshar, M.; Mofatteh, S. Biochar for a sustainable future: Environmentally friendly production and diverse applications. *Results Eng.* **2024**, *23*, 102433. [CrossRef]
88. Yaashikaa, P.R.; Kumar, P.S.; Varjani, S.; Saravanan, A. A critical review on the biochar production techniques, characterization, stability and applications for circular bioeconomy. *Biotechnol. Rep.* **2020**, *28*, e00570. [CrossRef]
89. Tijjani Usman, I.M.; Ho, Y.C.; Baloo, L.; Lam, M.K.; Sujarwo, W. A comprehensive review on the advances of bioproducts from biomass towards meeting net zero carbon emissions (NZCE). *Bioresour. Technol.* **2022**, *366*, 128167. [CrossRef]
90. Deng, B.; Yuan, X.; Siemann, E.; Wang, S.; Fang, H.; Wang, B.; Gao, Y.; Shad, N.; Liu, X.; Zhang, W.; et al. Feedstock particle size and pyrolysis temperature regulate effects of biochar on soil nitrous oxide and carbon dioxide emissions. *Waste Manag.* **2021**, *120*, 33–40. [CrossRef]
91. Scherdel, C.; Reichenauer, G.; Wiener, M. Relationship between pore volumes and surface areas derived from the evaluation of N2-sorption data by DR-, BET- and t-plot. *Microporous Mesoporous Mater.* **2010**, *132*, 572–575. [CrossRef]
92. Tomczyk, A.; Sokołowska, Z.; Boguta, P. Biochar physicochemical properties: Pyrolysis temperature and feedstock kind effects. *Rev. Environ. Sci. Biotechnol.* **2020**, *19*, 191–215. [CrossRef]
93. Jaswal, A.; Singh, A. Biochar Characteristics and its Effect on Soil Physico-chemical Properties. *Ann. Biol.* **2018**, *34*, 275–280.
94. Campion, L.; Bekchanova, M.; Malina, R.; Kuppens, T. The costs and benefits of biochar production and use: A systematic review. *J. Clean. Prod.* **2023**, *408*, 137138. [CrossRef]

95. Yang, Y.; Sun, K.; Han, L.; Chen, Y.; Liu, J.; Xing, B. Biochar stability and impact on soil organic carbon mineralization depend on biochar processing, aging and soil clay content. *Soil Biol. Biochem.* **2022**, *169*, 108657. [CrossRef]
96. Waheed, A.; Xu, H.; Qiao, X.; Aili, A.; Yiremaikebayi, Y.; Haitao, D.; Muhammad, M. Biochar in sustainable agriculture and Climate Mitigation: Mechanisms, challenges, and applications in the circular bioeconomy. *Biomass Bioenergy* **2024**, *193*, 107531. [CrossRef]
97. Deshoux, M.; Sadet-Bourgeteau, S.; Gentil, S.; Prévost-Bouré, N.C. Effects of biochar on soil microbial communities: A meta-analysis. *Sci. Total Environ.* **2023**, *902*, 166079. [CrossRef]
98. Martiny, T.R.; Avila, L.B.; Rodrigues, T.L.; Tholozan, L.V.; Meili, L.; de Almeida, A.R.F.; da Rosa, G.S. From waste to wealth: Exploring biochar's role in environmental remediation and resource optimization. *J. Clean. Prod.* **2024**, *453*, 142237. [CrossRef]